Colloids and Surfaces A 607 (2020) 125498

Contents lists available at ScienceDirect

Colloids and Surfaces A

journal homepage: www.elsevier.com/locate/colsurfa

Fabrication of superhydrophobic coatings for corrosion protection by electrodeposition: A comprehensive review

Jianguo Liu*, Xiuting Fang, Chengyuan Zhu, Xiao Xing, Gan Cui*, Zili Li

Shandong Key Laboratory of Oil & Gas Storage and Transportation Safety, College of Pipeline and Civil Engineering, China University of Petroleum (East China), Qingdao 266580, China

GRAPHICAL ABSTRACT

ARTICLE INFO

Keywords:
Superhydrophobic coatings
Electrodeposition
Anti-corrosion
Crystal modifiers
Durability

ABSTRACT

In recent years, superhydrophobic materials have shown tremendous industrial application value in many fields. Especially in the field of anti-corrosion, the superhydrophobic coating can capture the air to form many "air bags" on the surface of the substrate, so it has a strong water-repellent ability, thus isolating the corrosion media and achieving remarkable anti-corrosion performance. Various preparation technologies of superhydrophobic coatings have been proposed, but each has its own defects. As a relatively mature industrial processing method, electrodeposition shows unique advantages. However, there are few reviews on the preparation of anticorrosive superhydrophobic coatings by electrodeposition till now. In this paper, the general theory of superhydrophobic surface, including factors affecting wettability and theoretical wetting models, is firstly reviewed. Secondly, the mechanism, application status and anti-corrosion performance of superhydrophobic coatings prepared by metal electrodeposition, non-metallic electrodeposition, and composite electrodeposition are summarized in detail, respectively. The internal mechanism of process conditions, especially crystal modifiers, to regulate the coating morphology is described. Moreover, new developments over the years in electrodeposition such as pulse electrodeposition, magnetic field-induced electrodeposition, ultrasonic-assisted electrodeposition for the fabrication of superhydrophobic coatings are also presented. Finally, the deficiency of this technology is pointed out, and the future research directions of improving the durability of superhydrophobic coatings are proposed.

1. Introduction

Since the 1970s, people get inspiration from the self-cleaning phenomenon of lotus leaves, begin to study superhydrophobicity [1]. With the deepening of research, various superhydrophobic surfaces have been prepared and preliminarily applied in self-cleaning [2], anti-corrosion [3], oil-water separation [4], anti-ice and anti-fog [5], drag reduction [6] and other aspects [7], showing great industrial potential.

* Corresponding authors at: No. 66, West Changjiang Road, Huangdao District, Qingdao, China.
E-mail addresses: liujianguo@upc.edu.cn (J. Liu), chennacuigan@163.com (G. Cui).

https://doi.org/10.1016/j.colsurfa.2020.125498
Received 6 July 2020; Received in revised form 21 August 2020; Accepted 22 August 2020
Available online 30 August 2020
0927-7757/ © 2020 Elsevier B.V. All rights reserved.

Metal corrosion causes serious waste of resources, economic losses, and safety risks worldwide [8]. According to statistics, the annual cost of corrosion can account for 4 %–5 % of the GNP [9]. If a superhydrophobic coating is prepared on metal surface, it can effectively isolate the metal from the corrosive media due to its strong water-repellent ability, thereby significantly reducing the corrosion rate [10].

The so-called superhydrophobic surface refers to the surface with static water contact angle (WCA) greater than 150° [11], and some literatures suggest that the sliding angle (SA) should be less than 10° at the same time [12,13]. The wettability of the material surface is related to its surface energy and surface morphology. Therefore, there are two methods to prepare the superhydrophobic surface: one is the "top-down" method to construct proper micro-nano structure on the surface of the hydrophobic material; the other is the "bottom-up" method, in which the surface with micro-nano structure is modified with low surface energy materials [14]. Under the guidance of these two ideas, a variety of technologies for preparing superhydrophobic coatings have been developed, such as chemical etching [15,16], plasma etching [17,18], anodizing [19,20], electrospinning [21,22], sol-gel [23–27], etc. It is found that the combination of various methods can increase the hydrophobicity of the surface to a greater extent. For example, reference [28] reported a novel method to fabricate superhydrophobic coatings on copper by combining shot peening, dislocation etching, and stearic acid treatment. Shot peening can increase the surface roughness and the adsorption of stearic acid. Etching is conducive to the formation of micro-nano hierarchical structure, and chemical treatment can evidently reduce the surface energy, all of which are beneficial to improve hydrophobicity. Nevertheless, some of these technologies may require expensive equipment and raw materials which are even toxic to the environment and human health. Besides, the preparation process of some technologies is complex and difficult to control, or the preparation efficiency is low. These defects make it difficult for them to achieve large-scale industrial applications.

Electrodeposition has been used in automotive decoration, metal protection, and other industrial fields for a long time, but it has been gradually applied in the preparation of superhydrophobic coatings in recent years. Compared with other technologies for preparing superhydrophobic coatings, electrochemical deposition shows great advantages [29]: (1) Electrodeposition technology is mature, and has been widely used in the preparation of composite coatings [30], nanomaterials [31] and so on; (2) The required equipment is simple, and only suitable power supply, electrode materials and electroplating baths are usually required; (3) The process is simple and easy to control, so the cost is low; (4) The surface morphology of the coating can be easily controlled by adjusting parameters such as voltage, current, and deposition time, and the process conditions are repeatable; (5) It is not limited by the shape and size of the matrix so that it can be implemented on the surface of various complex components; (6)The preparation efficiency is high and batch preparation can be realized. Because of the above advantages, the preparation of superhydrophobic coatings by electrodeposition has great potential for large-scale industrial applications.

The electrodeposition simply refers to the process in which metal ions (or complex ions) move directionally in the electrolyte and are reduced on the cathode surface under the condition of an external power supply. Then the corresponding metal or alloy deposit on the cathode [32]. By controlling the process conditions, a reasonable microstructure can be constructed on the surface of the substrate so that the superhydrophobic effect can be achieved by the one-step method [33–35]. In some other cases, secondary modification with low surface energy substances is required [36]. With the development of electrodeposition technology, nonmetallic electrodeposition, composite electrodeposition [37,38], pulse electrodeposition [39–41], and jet electrodeposition [42–49] have been gradually applied in the preparation of superhydrophobic coatings on the basis of traditional single metal DC electrodeposition. Many unexpected results have been achieved by combining electrodeposition with ultrasonic technology [50–55] and magnetic field induced technology [56–60], which will be covered in detail in later sections.

This paper pays attention to the application of superhydrophobic coatings in the field of corrosion protection and is divided into five parts. The first part introduces the factors affecting wettability and theoretical wetting models. The second part reviews the mechanism, application situation, and the anti-corrosion performance of superhydrophobic coatings by electrodeposition technology, including metal electrodeposition, non-metal electrodeposition, and composite electrodeposition. Then the influence of crystal modifiers, current density, and deposition time on hydrophobicity and corrosion resistance was shown in the third part, followed by an introduction of the new development of electrodeposition technology for preparing anticorrosive superhydrophobic coatings. Eventually, the shortcomings of this technology and research directions to improve corrosion resistance and durability are pointed out.

2. Theory of superhydrophobic surface

2.1. Factors affecting wettability

2.1.1. Surface tension and surface free energy

Wettability is an essential property of a solid surface, which reflects the spreading ability of droplets on it. On the surface of some substances, droplets spread rapidly to form a liquid film, showing strong hydrophilicity, while on other solid surfaces, such as lotus leaves, droplets tend to remain spherical shape and easily roll off the solid surface, showing hydrophobicity. Generally, WCA equal to 90° is regarded as the dividing line of wettability. More specifically, WCA less than 90° is hydrophilic, otherwise, it is hydrophobic [61,62].

According to the theory of Shirtcliffe et al. [63], the wettability of droplets on a solid surface depends partly on the relative magnitude of gravity and surface tension. The attraction and repulsion among molecules inside the liquid cancel each other out so that the molecules are finally in a state of force balance. And the number of molecules is small in the thin layer on the liquid surface, so that these molecules are attracted from the inside of the liquid, and the force causes the droplets to tend to shrink inward. Conversely, the gravity tends to cause the droplets to spread. Therefore, when the surface tension is dominant, the droplets will remain nearly spherical. On the contrary, when the droplet size increases and gravity gradually dominates, the droplets will spread out.

Other researchers have proposed that surface free energy is an important factor affecting the wettability of a solid surface [64–66]. Surface molecules are less involved in chemical bonding because they are exposed to the outside, so compared with molecules inside the liquid, surface molecules have higher potential energy, which causes the generation of surface free energy [29]. In the field of thermodynamics, surface tension and surface energy are two different concepts [67], but they are closely related. The former represents the force acting on the unit boundary line (N/m), and the latter represents the change of Gibbs free energy with the increase of unit surface area (J/m^2) [68], both of which have the same dimension and describe the interface properties from the perspective of "force" and "energy" respectively. Especially under the condition of thermodynamic equilibrium, that is, when the pressure and temperature of the system are constant, the two values can be considered equal [69]. Studies show that lower surface energy is beneficial to enhance hydrophobicity. Silanes [2,15,70,71] and fluorocarbons [72,73] are common low surface energy materials, so they are widely used to prepare superhydrophobic coatings.

2.1.2. Surface morphology

Even though many substances are hydrophilic themselves, they can still achieve a hydrophobic effect by constructing suitable surface morphology, which fully demonstrates that wettability is not only

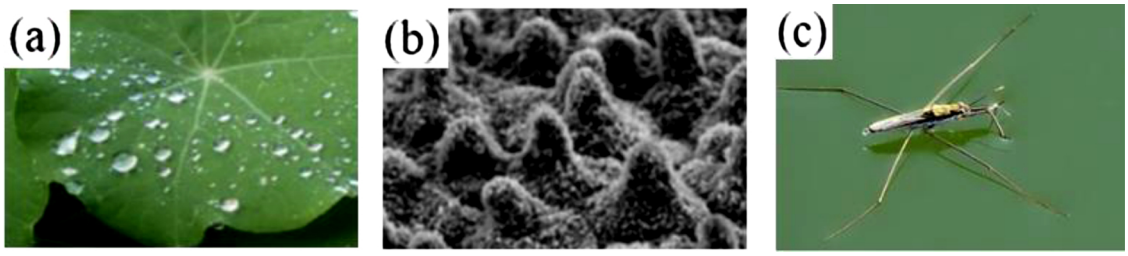

Fig. 1. Superhydrophobic phenomena in nature: (a) Self-cleaning effect of lotus leaves; (b) The micro-nano mastoid structure on the surface of lotus leaves; (c) A water strider floating on the surface of water.

affected by surface tension/surface energy but also affected by surface morphology. For example, nickel itself is a hydrophilic metal. However, many researchers have successfully prepared superhydrophobic nickel coatings on the different matrix by various means [74–76], and scanning electron microscope (SEM) observations have proved that micron and nanometer hierarchical structures play a crucial role in the superhydrophobicity. A large amount of air is trapped between these micro-nano bulges to form "air bags" [73], making it difficult for droplets to wet so that the superhydrophobic coating can achieve good anti-corrosion effect.

There are also many interesting superhydrophobic phenomena in nature. The reason why the lotus leaf has self-cleaning effect is that a layer of waxy papillae with a diameter of 5 − 9 μm is distributed on its surface, and these papillae are densely covered with villi with a diameter of about 120 nm [77,78], as shown in Fig. 1 (a) and (b). The water strider can walk freely on the water surface, as shown in Fig. 1 (c), because its legs are distributed with a large number of directional micro- bristles and nano-grooves. It also secretes a layer of keratin wax with low free energy on the legs. The above facts prove the comprehensive effect of surface chemical properties and micro-morphology on wettability.

2.2. Theoretical wetting models

2.2.1. Classic wetting model

The theoretical study of surface wettability dates back to the early 19th century. In 1804, Thomas Young, a British scientist, proposed the relationship between the WCA and the surface tension on a smooth and homogeneous surface and gave the Young's equation [79]:

$$\cos\theta = (\gamma_{SV} - \gamma_{SL})/\gamma_{LV} \tag{1}$$

where γ_{SV} 、 γ_{SL} and γ_{LV} represent the interfacial tension between solid-gas, solid-liquid, and liquid-gas, respectively, and θ is the equilibrium contact angle or intrinsic contact angle of water droplets on the solid surface. But the equation is only applicable to an ideal surface that is completely smooth, chemically uniform, and inelastic, as shown in Fig. 2 (a). Obviously, such a surface does not exist in reality. On this basis, Wenzel put forward the Wenzel model [80], in which the droplet will completely immerse in the small grooves of the surface when it contacts the rough surface, making the actual contact area larger than the apparent contact area, as shown in Fig. 2 (b), and the contact angle is given by Eq. (2).

$$\cos\theta_W = r\cos\theta \tag{2}$$

where r is called roughness factor equal to the ratio of the actual contact area to the apparent area between the droplet and the rough surface. Obviously, the value of r is greater than 1, that is, the roughness plays a "magnifying" effect on wettability. For a hydrophilic surface, increasing the roughness will make the surface more hydrophilic, while for the hydrophobic surface, increasing the roughness will help to improve its hydrophobicity. However, the Wenzel's model is still only applicable to surfaces with uniform composition. As a result, the Cassie-Baxter model [81] was proposed, in which the droplet doesn't immerse in the surface grooves but is located on a composite surface composed of gas and solid, as shown in Fig. 2 (c). In this case, the contact angle can be expressed by formula (3):

$$\cos\theta_{CB} = f_1\cos\theta_1 + f_2\cos\theta_2 \tag{3}$$

In the formula, f_1 and f_2 represent the ratio of the contact area of component 1 and component 2 to the total contact area, respectively, and the sum of them is 1; θ_1 and θ_2 refer to the apparent contact angle of component 1 and component 2, respectively.

Since the establishment of the above three wetting models, they have been widely accepted and become the theoretical basis for studying the wetting behavior of droplets [82]. However, it is undeniable that the above three models have their own limitations and cannot adequately describe all the wetting behavior.

2.2.2. Other wetting models

Because of the limitations of classic wetting models, some new wetting models were subsequently proposed, especially with the understanding of the micro-nano structure of the superhydrophobic surface. Many scholars have studied the wetting behavior of droplets on the surface with such dual-scale structures.

Marmur [83,84] proposed a compound model based on the Wenzel model and the Cassie-Baxter model. For Marmur's model, the droplets will be partially inserted into the air cushion, as shown in Fig. 2 (d). This model is a transition state between the Wenzel model and the Cassie-Baxter model, and Bico et al. [85] also theoretically proved the possibility of transition between these two states.

Wang et al. [86] proposed that there are five wetting states of liquid droplets on a solid surface, namely Wenzel's state, Cassie's state, the transitional state between Wenzel's and Cassie's states, the "Gecko" state and the "Lotus" state. Cha et al. [87] considered that there are four kinds of wetting states on the surface with micro-nano dual-scale structures, namely, Cassie-Cassie mode, Cassie-Wenzel mode, Wenzel-Cassie mode, and Wenzel-Wenzel mode. They theoretically gave the formulas for calculating the contact angles of these four wetting modes according to the change of free energy caused by the small displacement of the contact line, but the model did not consider the effect of nanostructures distributed on the side wall of microstructures on wettability. Wu et al. proved that the nanostructure on and on the side of the microstructure would affect the wettability [88]. At the same time, they also proposed that there were four stable wetting states and five transition states of droplets on the surface of micro-nano dual-scale structure, and derived equations for calculating the apparent contact angle of each state from the point of thermodynamics [89]. Bhushan and Nosonovsky [90] pointed out that there were 9 wetting states when droplets were on the surface of the micro-nano dual-scale structure, but the conditions and the calculation method of contact angle of each state were not described.

The above models are based on the assumption that the droplet size is much larger than the surface structure size, but when the droplet size reaches the micron level or less, these models will no longer be applicable [91]. In this case, the effect of line tension [92] can not be ignored, and the contact angle is determined by the Neumann-Boruvka

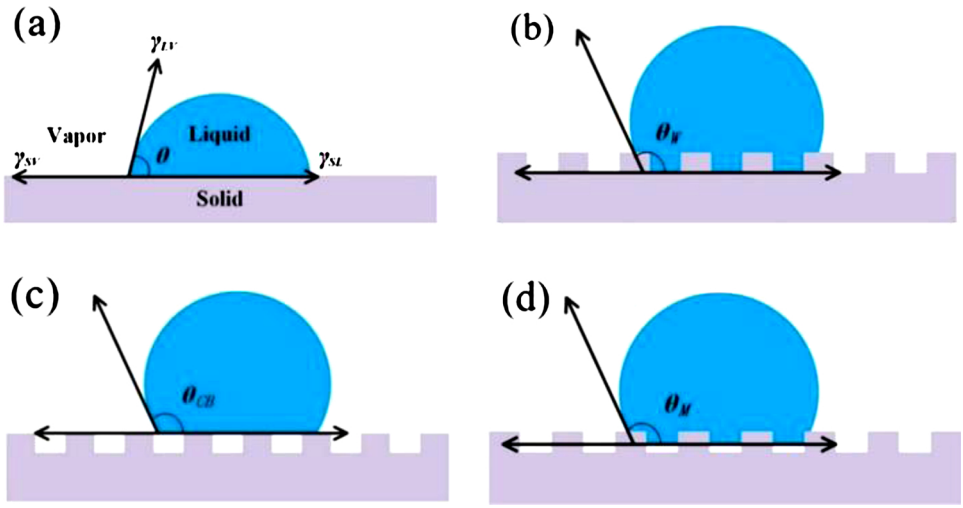

Fig. 2. Schematic of theoretical wetting models: (a) Young's model; (b) Wenzel model; (c) Cassie-Baxter model; (d) Marmur model.

equation [93]:

$$\cos\theta_{NB} = \frac{\gamma_{SV} - \gamma_{SL}}{\gamma_{LV}} - \frac{\Gamma}{\gamma_{LV} a} \quad (4)$$

where Γ is line tension and a is contact radius. However, due to the limited measurement technology and difficulties in sample preparation [92], there is a great difference between the theoretical and experimental values of line tension reported in literatures [94–96].

In addition, the change of temperature and other factors may also lead to the change of wetting state [91,97]. To sum up, the wetting behavior of droplets on a real surface is complex, and the traditional three classical wetting models are not enough. Although some new wetting models have been proposed, they have not been widely recognized in this field. A correct and comprehensive model needs to be established, and the micro-wetting mechanism of droplets needs to be further studied.

3. Anticorrosive superhydrophobic coatings prepared by electrodeposition

According to the different deposition media, electrodeposition can be divided into metal (and its compounds) electrodeposition, non-metallic electrodeposition and composite electrodeposition. With the preparation of superhydrophobic surface becoming a research hotspot, many researchers have made great attempts based on these three methods, and successfully fabricated superhydrophobic coatings on various substrates, which achieved remarkable anti-corrosion effect.

3.1. Metal electrodeposition

3.1.1. Mechanism of metal electrodeposition

Metal electrodeposition is a primary subject in the field of electrochemistry. Briefly, it is the process of metal ions discharging at the interface between electrode and solution to form a new metal phase under the action of the electric field. Since the 19th century, a large number of observations and studies have been carried out on the process of metal electrodeposition, and a relatively mature theory has been formed [98].

Metal electrodeposition can be divided into two stages. The first stage is the ion transport from the electrolyte to the electrode surface and discharge, and the second stage is the atom into the lattice and crystal growth [99,100]. The former conforms to the basic law of cathodic reduction in general aqueous solutions, but the kinetic law of cathodic reduction is more complicated due to the continuous changes in the surface state of the electrode. The latter accords with the fundamental law of the crystallization process while it is also affected by the electric field at the cathode interface. Therefore, the two processes influence each other, resulting in the complexity of the metal electrodeposition process. Specifically, it can be divided into the following four steps [101–103]: (1) The mass transfer process in the liquid phase, that is, the reaction particles in the solution such as hydrated ions and complex ions migrate to the electrode surface by electromigration, convection, and diffusion; (2) Pre-conversion process in which the particles to be reacted near the electrode undergoes a chemical conversion reaction, such as the decrease of the hydration degree of metal hydration ions or the rearrangement of water molecules and the reduction in the coordination number of metal complexes; (3) Charge transfer process means that the reaction particles get electrons to become adsorbed atoms at the interface of electrode and solution. The second and third steps can be expressed as ; (4) Electro-crystallization process. It is generally considered that there are two forms of this process, one is that the newborn adsorption atoms produced by cathodic reduction gather to form crystal nuclei which gradually grow to form crystals, the other is that the newborn adsorption atoms spread on the surface of the electrode, then reach a specific position and enter the lattice to continue to grow on the original metal lattice [104,105].

Among the above four steps, the step with the highest resistance and the slowest rate becomes the rate-determining step of electrodeposition, which varies with the difference of electrochemical systems and process conditions. The development of observation technology and electrochemical measurement technology provides convenience for studying the metal deposition process of specific systems. Kelber et al. [106] used cyclic voltammetry, current-time transient measurement, and atomic force microscope to observe in situ the electrodeposition process of Cu on Ru (0 0 1) surface in sulfuric acid solution. The observed data showed that the deposition/crystallization process of Cu did not completely conform to the classical two-dimensional and three-dimensional nucleation model [107,108], and the growth of copper crystals showed distinct anisotropy. Sotskaya et al. [109,110] studied the electrodeposition and crystallization of Ni on the surface of Cu in different systems and calculated the main kinetic parameters of the nucleation process. It was found that the crystallization process of Ni satisfied the instantaneous nucleation mechanism. Wasekar et al. [111] established a mathematical model of the crystal size of Ni in the presence of boron, sulphur, and phosphorus by analyzing the mass transfer process at the cathode-electrolyte interface. It was found that the size of deposited particles was directly proportional to the current efficiency and deposition rate, and inversely proportional to the current density and the content of metals (B, S, P) in the coating.

In a word, with the application of electrodeposition technology to

more and more fields, the electrochemical systems constructed are becoming more and more complex. Using a variety of technical means, we can better study the similarities and differences of electrodeposition processes in different systems.

3.1.2. Anti-corrosion performance

A typical electrodeposition method requires three processes: pre-treatment, electrodeposition and post-treatment. Firstly, the substrate needs to be polished to a certain roughness, and the surface oxide layer is removed, and then ultrasonically cleaned in acetone and ethanol solution to initially degrease. In order to achieve a better degreasing effect, it is usually necessary to wash the matrix in alkaline washing liquid for a period of time, otherwise, incomplete degreasing will make it difficult for the deposition layer to combine closely with the matrix. Finally, the substrate is activated by dilute acid and then immersed in the electrolyte for the electrodeposition process. After the electrodeposition, some samples only need to be washed with deionized water and dried to achieve the superhydrophobic effect, and some require heat treatment [112], or exposed to the air for a period of time [59], some others require surface modification with low surface energy substances [36].

The superhydrophobicity of the prepared coating prevents the corrosion medium from adhering to the surface of the substrate to achieve excellent anti-corrosion performance. In recent years, researchers worldwide have carried out many attempts, and the superhydrophobic coatings have been successfully prepared on the surface of common metals and their alloys, such as iron, copper, aluminum, magnesium, and so on, and a good anti-corrosion effect has been achieved.

3.1.2.1. Superhydrophobic coatings on the steel substrate. Steels have become the most widely used metal in the industrial field because of their low price and excellent mechanical properties, but the corrosion of steel is always inevitable, so the anti-corrosion research of steel has never stopped [113]. The preparation of superhydrophobic coatings undoubtedly provides a new answer for the anti-corrosion of steel.

Li et al. [36] prepared a superhydrophobic zinc coating on the surface of X60 steel by electrodeposition. Using $ZnSO_4$ solution as the electrolyte, they first electrodeposited at the current density of 4 A/dm^2 for 20 min then at the current density of 9 A/dm^2 for 3 min under the condition of pH = 4 and temperature of 25 ˚C, and finally fluorinated with perfluorooctanoic acid ethanol solution. The micro crater-like structure was formed on the surface of the substrate with the WCA reaching 154.21˚ and the SA less than 5˚. The superhydrophobic zinc coating could not only play a hydrophobic role but also had a cathodic protection effect, which provided double protection to the substrate. Meanwhile, after 80 days of exposure to the atmosphere, the contact angle was still above 150˚.

Liu et al. [114] immersed 316 l stainless steel in an electrolyte solution composed of $NiCl_2$, H_3BO_3, and $CuCl_2$ to prepare a Cu-Ni superhydrophobic coating at a current density of 8 A/dm^2 for 20 min. It could be found that a dense branch-like structure was formed on the surface of the matrix, and the surface morphology of the matrix before and after deposition was shown in Fig. 3 (a) and (b). The size of the trunk structure was about 4 − 8 μm, and the fine dendrite structure was about 300 − 600 nm. After being modified by myristic acid, the WCA and SA were 161.27˚ and 7.8˚, respectively. The anti-corrosion performance of the coating was investigated by electrochemical test in 3.5 wt. % NaCl solution and the results were shown in Fig. 3(c) and (d). It was verified that the superhydrophobic Cu-Ni coating exhibited lower corrosion current density, higher corrosion potential, and larger impedance modulus, corresponding to better corrosion resistance. And the anti-corrosion efficiency of the coating reached 99 % calculated by Eq. (5):

$$\eta = \frac{I_{corr,sub} - I_{corr,coated}}{I_{corr,sub}} \times 100\% \quad (5)$$

As a result, the anti-corrosion effect was very significant. The contact angle of the coating had no obvious change after being exposed to air for 6 months and immersed in a strong acid solution with pH = 1 for 12 h, but after soaking in a strong alkaline solution with pH = 14 for 4 h, the superhydrophobic effect dropped sharply.

3.1.2.2. Superhydrophobic coatings on the copper substrate. Copper is widely used in electronics, electric power, electricity, and some emerging high-tech fields because of its excellent electrical conductivity, thermal conductivity, and ductility [115–117]. Although the activity of copper is less than that of iron, studies have shown that copper is very prone to corrosion in a humid environment with the presence of Cl^- [118]. Therefore, if a protective film with hydrophobic and self-cleaning effect is prepared on the surface of copper, it will effectively isolate the adsorption and penetration of Cl-.

Khorsand et al. [119] prepared superhydrophobic nickel coatings on copper substrates by electrodeposition at 60 ˚C and pH = 4 in an electrolyte solution composed of $NiCl_2$, H_3BO_3, and $C_2H_{10}C_{l2}N_2$. It was found that the nickel coating deposited at the current density of 20 mA/cm^2 for 600 s and then at the current density of 50 mA/cm^2 for 60 s exhibited the best superhydrophobic property with the WCA reaching 155˚. SEM results showed that the coating was covered by micro-nano dual-scale pineal structures, more specifically, nano-scale protrusions were densely distributed on the micron nickel cone. The results of electrochemical impedance spectroscopy and polarization curves suggested that the superhydrophobic coating had good corrosion resistance in 3.5 wt.% NaCl solution.

3.1.2.3. Superhydrophobic coatings on the Mg alloy substrate. Magnesium is one of the most abundant elements on earth. Magnesium and its alloys are widely used in aerospace, electronic equipment, automobile and other fields because of high strength, low density, excellent electrical conductivity and electromagnetic shielding [120]. However, magnesium has more negative potential and higher activity than iron, copper and aluminum, thus facing a high risk of corrosion [121,122].

Liu et al. [123] prepared a superhydrophobic CeO_2 coating with the WCA equal to 150˚ on the surface of AZ31B magnesium alloy by electrodeposition under the condition of 0.65 mA/cm^2 for 60 min. After being modified with stearic acid, the WCA of the coating increased to 158˚, and the surface was covered by petal-like nanosheets. The anti-corrosion efficiency of the sample could still reach about 90 % after soaking in 3.5 % NaCl solution for 48 h, meaning that the coating gave the substrate good corrosion protection. When the coating was exposed in the atmosphere for 60 days and contacted with water droplets with pH of 1–13, the WCA maintained more than 150˚, but after immersed in NaCl solution for 100 h, the hydrophobic effect began to decrease sharply. In addition, the superhydrophobic effect disappeared after being dragged by 140 cm with a weight of 50 g on the sandpaper of 600 grit, and the coating cannot provide corrosion protection as a result.

If the low surface energy substances were directly added to the electrolyte solution, the metal ions could react with the functional groups of these substances in the process of electrodeposition, and metal compounds with low surface energy are formed directly on the surface of the cathode. In this way, a good hydrophobic effect can be achieved without surface modification after electrodeposition. For example, Zheng et al. [124] used ethanol solution of magnesium nitrate and stearic acid as the electrolyte and electrodeposited for 30 min under constant voltage (30 V) to fabricate superhydrophobic coatings on the surface of AZ31 magnesium alloy by the one-step method. Through X-ray photoelectron spectroscopy, Fourier Transform Infrared Spectrometer and Energy Dispersive Spectrometer, the coating was mainly composed of magnesium stearate and a small amount of magnesium oxide, and the maximum WCA was 156.2 ± 4.9˚. The corrosion current density of the coating in 3.5 % NaCl solution was much lower than that of the bare substrate, and the WCA remained about 150˚ after soaking for seven days, which meant that the coating could provide

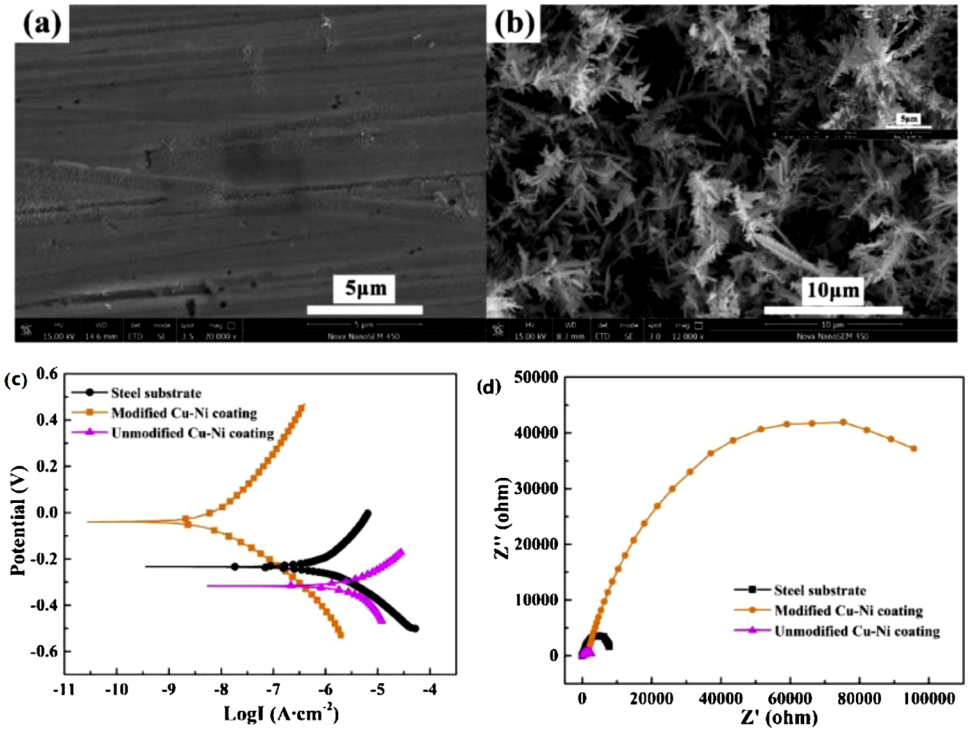

Fig. 3. SEM images of (a) bare steel matrix and (b) superhydrophobic coating, and (c) Potentiodynamic polarizaiton curves and (d) Nyquist plots [114].

relatively lasting corrosion resistance.

3.1.2.4. Superhydrophobic coatings on the aluminum alloy substrate. Aluminum and its alloys are widely used in industrial fields because of their high strength, low density, strong electrical, thermal conductivity and good processability. Although Al easily forms an oxide film in the air and provides protection to a certain extent, the corrosion resistance of this film is poor. Once it contacts with acidic or alkaline media, the film is easy to dissolve and cause severe pitting corrosion, crevice corrosion and other local corrosion.

Xu et al. [125] prepared nickel stearate/nickel hydroxide superhydrophobic films on chemically cleaned aluminum alloy substrate by one-step electrodeposition using ethanol solution containing nickel nitrate hexahydrate and stearic acid (SA) as the electrolyte. The results showed that when the molar ratio of Ni^{2+}/SA was 0.4, the surface of the film reached the best hydrophobic performance with the WCA of 160 ± 1° and the contact angle hysteresis value of 2.1 ± 1°. SEM images proved that the formation of micro-nano dual-scale cauliflower-like structures on the surface was the main reason for its superhydrophobicity. The polarization curves and the resulting polarization resistance and current density of the coatings are shown in Fig. 4. The corrosion resistance of the substrate covered with superhydrophobic coating calculated by polarization curves was about 280 times higher than that of the substrate without coating. However, the durability of the prepared coating had not been reported in this literature.

Cathodic electrodeposition is the most widely used form; however, in some cases, anticorrosive superhydrophobic coatings can be obtained by anodic electrodeposition. For example, Zhang et al. [126] prepared an anticorrosive superhydrophobic coating on the surface of aluminum alloy by anodic electrodeposition in the mixed solution of ferric chloride and myristic acid with aluminum alloy as the anode. During electrodeposition, Al was firstly oxidized to Al^{3+} and then combined with $CH_3(CH_2)COO^-$ from myristic acid to form aluminum myristate and deposited on the anode surface. Finally, the surface of the substrate was covered with micro-nano structure to form Danxia-landform-like morphology with a WCA of 155.1°. Through electrochemical tests, the corrosion potential of the matrix changed from −1.280 V to −0.869 V, and the corrosion current density was reduced by 85 %, demonstrating that a good corrosion protection effect was achieved.

In addition, the successful cases of preparing various superhydrophobic coatings on the substrate by metal electrodeposition in the past six years are listed in Table 1. In summary, various superhydrophobic coatings have been prepared on different substrates by metal electrodeposition to achieve a good anti-corrosion effect. However, in most cases, surface modification is required, and the hydrophobicity depends on the micro-nano dual-scale structure of the surface so that the wear resistance and durability of the coating need to be further improved.

3.2. Nonmetallic electrodeposition

It is not only metals that can be electrodeposited to form superhydrophobic coatings. Many nonmetals, especially some conductive polymers with low surface energy, can achieve superhydrophobic effect directly by one-step electrodeposition, which avoids secondary surface modification and expands the application of electrodeposition in the preparation of anticorrosive superhydrophobic coatings.

Xu et al. [137] prepared a series of polythiophene films (PL-PEDOT) on indium tin oxide (ITO) glass by electrodeposition, in which wettability could change from superhydrophilic to superhydrophobic. Initially, they used cyclic voltammetry to make the poly(3,4-ethylenedioxythiophene) (PEDOT) deposit on ITO electrode as the first superhydrophilic layer. Subsequently, the overlying hydrophobic ploy (2,2′-bithiophene) (PLTH) moieties with various electrodeposition charge (EC) were electrodeposited on the as-prepared PEDOT layer by applying a constant potential. As the EC of PLTH changed, the wettability of the coating surface continued to change, with the WCA from 0° to 150.4° gradually.

Many fluorine-containing carbon chains often have low surface energy, and they can be combined with specific organic substances through chemical reactions to synthesize some new hydrophobic substances, which can be used in electrodeposition to prepare superhydrophobic films. Darmanin et al. [138] used 3,4-ethyleneoxythiathiophenes (EOTT) as platform molecules to synthesize its

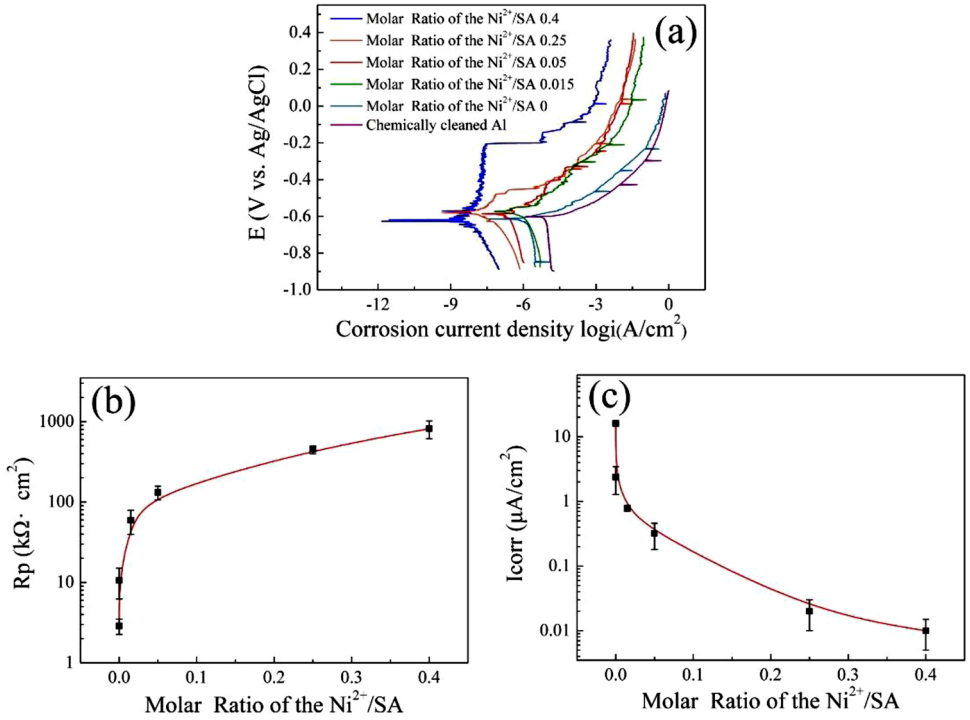

Fig. 4. (a) Potentiodynamic polarization curves, (b) the polarization resistance (R_p) and (c) corrosion current density (I_{corr}) of samples under various Ni^{2+}/SA molar ratios [125].

derivatives (EOTT-F_n) containing semifluorinated chain of different length. After electrodeposition, these derivatives were deposited on the surface of the gold substrate, and it could be found that when n was greater than 4, the surface was superhydrophobic with the contact angle above 158.9°. Thereafter, they synthesized a 3,4-ethylenedithiophene (EDOT) derivative containing a short fluorinated chain (C_4F_9) and a highly rigid methoxybenzothioate spacer [139]. Then the polymer monomer was added to various electrolyte to make them deposit on a gold plate via electrodeposition. After that, nanofibrous structures of different sizes were observed on the surface of the substrate, and the WCA was around 160°, which proved that the coating had achieved a very superhydrophobic effect.

Wang et al. [71] prepared the precursor solution by adding dodecyltrimethoxysilane (DTMS) to the mixed solution of ethanol and potassium nitrate. After full hydrolysis of the precursor solution, superhydrophobic DTMS silane films were prepared on the surface of low carbon steel by electrodeposition in a three-electrode system. Further study showed that the hydrophobic effect was the best when the deposition time was 300 s, and the applied potential was -1.3 V. At this time, the WCA was 152.9°, and the SA was only 3°. SEM observations revealed that the nanosheets were entangled with each other to form a walnut-like micro-bundle on the surface of the substrate. Potentiodynamic polarization curves of the prepared samples in 3.5 wt.% NaCl solution are shown in Fig. 5, based on this, the calculated corrosion current density of the substrate with superhydrophobic DTMS coating was reduced by three orders of magnitude compared with the bare

Table 1
Examples of superhydrophobic coatings by metallic electrodeposition.

Matrix	Coating	Electrolyte composition	Process conditions	WCA	SA	ref
Stainless steel	Ni	Plating solution: $NiCl_2$ + H_3BO_3 + lauryl sodium sulfate Modification : FAS-13	5A/dm^2	165°	1°	[127]
Stainless steel	Cu-Ni	$NiSO_4$ + $CuSO_4$ + Na_2SO_4 + NDM + dopamine hydrochloride	0.6A/cm^2(20 min), 35 °C	162 ± 1°	—	[128]
Mild steel	Ni-Cr	$NiCl_2$ + $CrCl_3$ Modification: myristic acid	6A/dm^2(10 min) + 15A/dm2 (20 s)	167.9 ± 2.4°	4.7 ± 0.8°	[129]
X90 steel	Cu-Zn	$ZnSO_4$ + $CuSO_4$ + NaOH + $C_4O_6H_4KNa$	2A/dm^2(60 min)	154.73°	6.5°	[130]
C45 steel	Fe	$FeCl_3$ + palmitic acid + ethanol	30 V(10 min)	160.5 ± 0.5°	2 ± 0.5°	[131]
H62 brass	Ni	Etching liquid: $FeCl_3$ Plating solution: $NiCl_2$ Modification : trichloro silane	Chemical etching(17 min) + 0.05A/cm^2(15 min), 35 °C+ Surface modification	159.5 ± 1.7°	3.3 ± 0.6°	[132]
Mg alloy	Cerium stearate	$Ce(NO_3)_3$ + stearic acid	30 V(10 min)	158.4 ± 0.9°	2°	[133]
Mg alloy	Cerium myristate	$Ce(NO_3)_3$ + myristic acid	20 V(10 min)	160.4 ± 0.7°	—	[35]
Be-Cu alloy	Copper stearate	$CuCl_2$ + HCl + stearic acid	5 V(10 min)	163 ± 4°	1.7 ± 0.2°	[134]
Copper	Aluminum stearate	AlOx + stearic acid	30 V(10 min)	161 ± 1°	2 ± 1°	[135]
Tin (Sn)	Zn/ZnO	$Zn(Ac)_2$ + HCl + KCl	−1.6 V (10 min) + annealed at 200 °C (10 min)	160°	1°	[136]

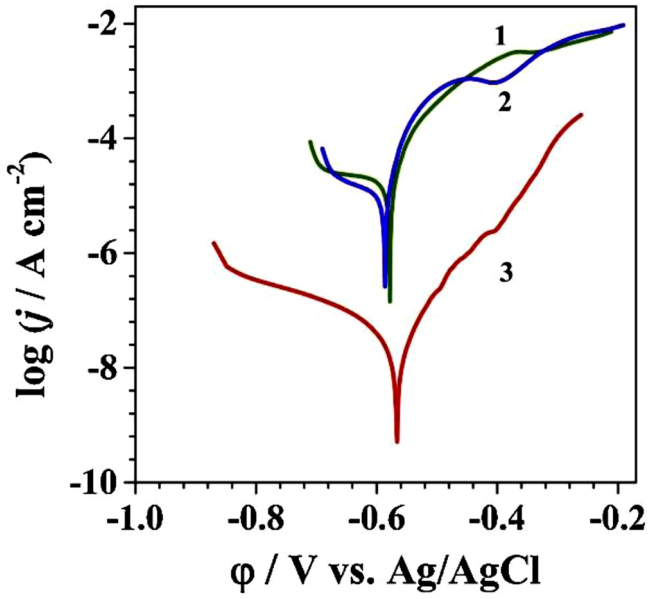

Fig. 5. Tafel plots of (curve 1) bare, (curve 2) traditional silanization treated and (curve 3) superhydrophobic DTMS surfaces coated MS substrates [71].

substrate, and the anti-corrosion efficiency was as high as 99.74 %. Although the thickness of the coating was only 3.7 μm, the protection efficiency was much higher than that of the superhydrophobic epoxy coating with a thickness of 30 μm [140]. The WCA of the coating began to decrease after soaking in NaCl solution for three days, however, remained relatively high at 134.9° after eight days of immersion and kept almost unchanged in the following year.

Further research found that DTMS firstly produced active silanol groups through hydrolysis in the precursor solution. During electrodeposition, water electrolysis and oxygen reduction produced OH^-, which effectively catalyzed the condensation process of silanol groups on the metal surface so that cross-linking structure and covalent binding (Si-O-Si and Si-O-Metal) were generated. As a result, DTMS was firmly bonded to the surface of the substrate, as shown in Fig. 6. The subsequent drying and curing process resulted in a micro-nano rough structure on the surface of the coating, and DTMS itself has lower surface energy, thus achieving superhydrophobicity and anti-corrosion effect by one-step electrodeposition.

Other successful cases of preparing various superhydrophobic surfaces by non-metallic electrodeposition are listed in Table 2. Overall, compared with metal electrodeposition, non-metal electrodeposition has less application in anticorrosive superhydrophobic coatings. In the process of preparation, there is often no need for secondary surface modification, but a good superhydrophobic and anti-corrosion effect can still be obtained. Nevertheless, the non-metals used often do not have mechanical strength, so poor stability and durability is still an urgent problem to be solved.

3.3. Composite electrodeposition

3.3.1. Mechanism of composite electrodeposition

Some particles with special properties are added to the electrolyte, and these particles will be co-deposited on the surface of the substrate together with the basic phase to form a composite coating, so that the coating not only has the characteristics of the basic phase, but also exerts the advantages of co-deposited particles. In this way, the composite coating obtains unique electrical conductivity, corrosion resistance, wear resistance, self-lubrication, and other properties. Thus, the coating possesses a wide range of industrial applications in aerospace, automotive engineering, textile, and general engineering [30]. The basic phases of deposition can be metals, alloys, conductive polymers and conductive ceramics, while the co-deposited particles can be spherical, layered, needle-shaped and other shapes of oxides, carbides, borides, nitrides, etc., with sizes ranging from micron and submicron to nanometer [146]. In the preparation of superhydrophobic coatings, the co-deposition of nanoparticles and metals is the most widely used.

Composite electrodeposition generally involves two processes: the good dispersion of particles in the electrolyte, and the co-deposition of particles with matrix metal ions [147]. Given these two processes, many scholars have established models of co-deposition since the 1970s. Guglielmi [148] described the role of adsorption and electrophoresis in co-deposition, which related the concentration of particles in composite coatings to the concentration of particles suspended in the liquid and electrode overpotential, but the model did not take into account mass transfer, particle entanglement, electroadsorption and electrokinetics [149]. It is generally believed that in the process of composite electrodeposition, the movement of solid particles from the plating solution to the cathode surface would be affected by two forces: (1) the flow of the bath made the solid particles suspend and move to the vicinity of the cathode, and (2) the solid particles reached the surface of cathode by electrophoresis under the action of electric field [150]. Therefore, the cathodic current efficiency and the dispersion ability of particles in the electrolyte solution are two critical factors affecting composite electrodeposition.

The model proposed by Celis et al. [151] has been widely accepted so far, in which the co-deposition of particles and the basic phase went through five steps, as shown in Fig. 7. Firstly, some nanoparticles are wrapped by surfactants and metal cations to form "ionic clouds". Then these ionic clouds and part of particles move towards the cathode through a hydrodynamic boundary layer (convection layer), which is usually less than 1 mm. Next, they diffuse through the concentration boundary layer (diffusion layer), which can reach hundreds of microns. After that, these particles pass through an electric double layer with a thickness of only a few nanometers and are adsorbed on the surface of the cathode, and finally, co-deposited along with the reduction of the metal cation. Subsequently, some new models were proposed. For example, Hwang et al. [152] analyzed the co-deposition mechanism of silicon carbide and cobalt and believed that the deposition rate was related to the electrode reaction, considering the liquid phase mass transfer. Fransaer et al. [153] observed the co-deposition process of spherical particles and metal on the rotating disk electrode, and expounded the effects of fluid velocity, particle concentration and current density on the particle deposition rate, but the model ignored the effect of Brownian motion.

The above models are often based on a certain deposition system, so their accuracy is limited. Simultaneously, the existing models do not consider the effect of particle inclusions on the electrocrystallization process. Typically, the deposition of particles on the surface of the matrix will change the area and morphology of the cathode, which will inevitably affect the electrocrystallization process [149]. The author suggests that adsorption, electrochemical factors, and hydrodynamic factors must be comprehensively considered to establish a more applicable composite electrodeposition model.

3.3.2. Anti-corrosion performance

Due to the fragility of the micro-nano structure, various superhydrophobic coatings prepared in the past generally have poor wear resistance. At the same time, if the surface of the substrate is modified with a layer of low surface energy substances, many of them are toxic and have low adhesion to the substrate, which leads to the loss of superhydrophobicity. So that such coatings cannot provide long-term corrosion protection to the matrix. With the help of electrodeposition technology to prepare composite coatings, these problems have been solved to some extent. Especially with the exploration of new materials such as graphene and carbon nanotubes, the application of composite electrodeposition in the preparation of superhydrophobic coatings has

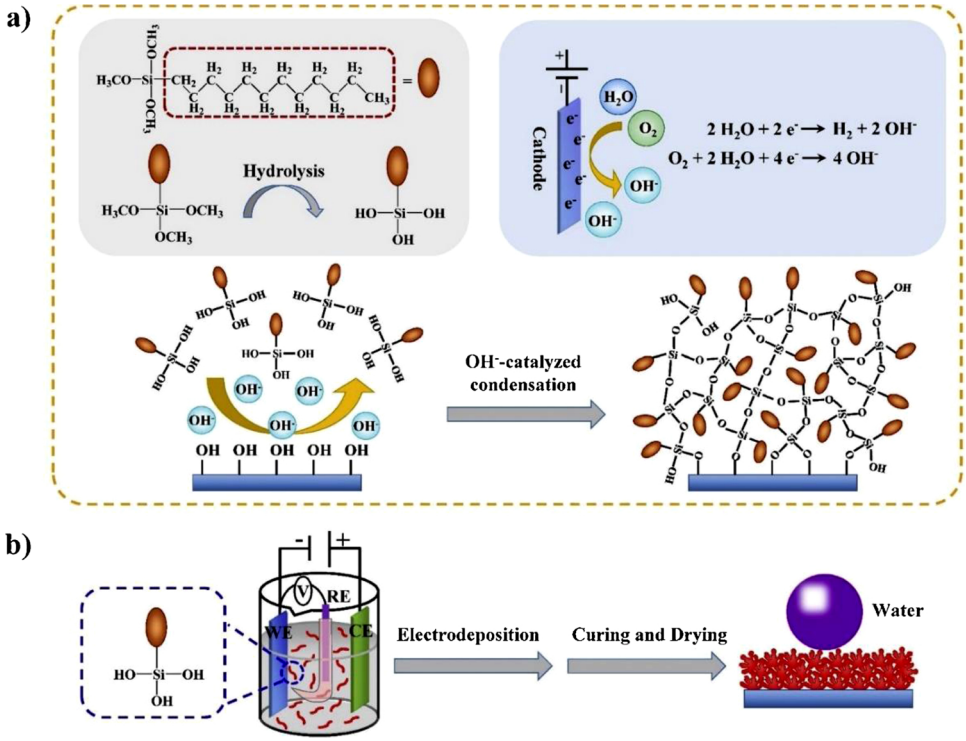

Fig. 6. Schematic illustration of (a) electrochemically catalyzed condensation reaction of DTMS and (b) electrodeposition of protective superhydrophobic DTMS films on the MS substrates [71].

been expanded.

3.3.2.1. Graphene-based composite superhydrophobic coatings. Since the 21 st century, graphene discovery has been regarded as one of the most brilliant achievements in the field of materials science [154]. As an emerging material, graphene itself has hydrophobicity and high specific surface area, and it also has excellent mechanical properties and electrical conductivity [155], exhibiting great application value in many fields. In recent years, many researchers have explored the application of graphene in superhydrophobic composite coatings.

Choi et al. [156] prepared petal-shaped Graphene/Nafion hybrid films by chemical method. The film had a good hydrophobic effect with the WCA up to 161°. However, the preparation of this coating required complex pretreatment. The mixed solution of graphene oxide (GO) and Nafion not only needed to be treated with hydrazine solution at 85 °C for 24 h, but also needed to be purified by dialysis for 1 week, making the preparation process extremely complicated. On the contrary, the preparation of superhydrophobic coatings containing graphene by composite electrodeposition is simple. Ding et al. [157] directly added multi-layer graphene to the bath containing Ni^{2+} and carried out electrodeposition at a current density of 20 mA/cm^2 for 5 min. After the modification of myristic acid, the WCA reached 160.4 ± 1.5° and the SA was as low as 4.0 ± 0.9°. SEM observation showed that nano-nickel conical arrays were randomly distributed on the micron graphene bulge. According to results of extrapolation based on polarization

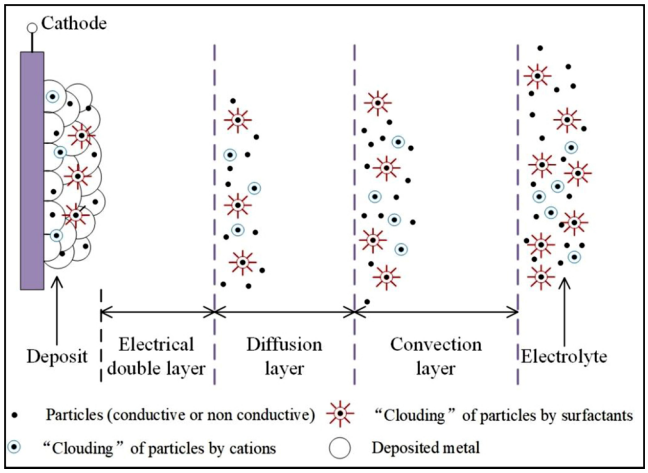

Fig. 7. The process of co-electrodeposition of particles and metal.

Table 2
Examples of superhydrophobic coatings fabricated by non-metallic electrodeposition.

Matrix	Coating	Electrolyte composition	Process conditions	WCA	SA	ref
Cotton fabric	SiO_2-OTEOS	Tetraethoxysilane (TEOS) + SDBS + HCl + Triethoxyoctylsilane(OTEOS)	15 V (10 min)	157.7°	——	[141]
ITO	Terthiophene(3 T)/3 T -initiator	Surface-initiated atom transfer radical polymerization (SI-ATRP)	0 ~ 1.2 V, a scan rate of 10 mV/s, 20 cycles	153 ± 2°	0°	[142]
ITO	Perfluoroalkyl alkyl pyrrole	——	1.25 V (300 s)	152.3°	No SA	[143]
Gold	PEDOT derivatives	——	100 mC/cm^2	159.4°	3.5°	[144]
Gold	Fluorinated polypyrene	Bu_4NClO_4 + anhydrous acetonitrile + pyrene monomers	−0.7 V to E^W (1.4 ~ 1.9 V), a scan rate of 20 mV/s	160°	1.0°	[145]

curves, the i_{corr} of the prepared superhydrophobic coating was only about 0.005 % of that of the bare substrate and the polarization resistance was approximately 1.88 × 10^4 times higher than that of the bare substrate, showing significant anti-corrosion effect. It is gratifying that the WCA of the coating didn't decrease obviously after 60 cycles of wear test at 1.0 kPa, proving that the coating had excellent wear resistance.

However, the graphene content in the coating prepared by the above method was still not high enough, and the surface modification was still needed. Bai et al. [158] improved the electrodeposition process by using the combination of Ni pre-deposition and an elevated current assistant approach. A new type of reduced graphene oxide (rGO)/Ni composite coating with pinecone-like micro/nanostructure was successfully prepared on stainless steel substrate, and the WCA and SA were 162.7 ± 0.8° and 2.5 ± 1.0°, respectively. After soaking in 3.5 % NaCl solution for 36 h, the anti-corrosion efficiency of the coating could still reach 99.98 % according to the results of polarization curves. Importantly, the WCA and SA of the coating decreased slightly but still maintained superhydrophobic after 100 cycles of mechanical abrasion test, demonstrating that the superhydrophobic coating obtained good mechanical stability.

3.3.2.2. Carbon nanotube-based composite superhydrophobic coatings. Since the discovery and naming of carbon nanotubes (CNTs) in 1991, this special one-dimensional nanostructured material has rapidly gained widespread attention [159]. Carbon nanotubes have unique physical and chemical properties, including high specific surface area, good lubricity, high hardness and wear resistance [160], making it an excellent choice for the preparation of superhydrophobic composite coatings.

Barthwal et al. [161] prepared ZnO/multi-walled carbon nanotubes (MWCNTs) composite coating on the copper mesh by sol-gel method, but the coating must be modified by PDMS to achieve superhydrophobicity. However, Zhou et al. [162] prepared MWCNTs-Ni/a-C: H composite coating on silicon substrate by one-step electrodeposition using nickel (II) acetylacetonate and MWCNTs methanol solution as the electrolyte solution. The preparation process of electrodeposition is shown in Fig. 8, which was facile and simple. And finally, the WCA of the coating was 158.89°, and the SA was only 1.99°. Under the weight of 100 g, the coating could still maintain superhydrophobicity after 20 wear cycles, exhibiting good wear resistance. In 3.5 % NaCl solution, the corrosion current density of the samples covered with the coating decreased significantly, which proved that the coating achieved a good anti-corrosion effect.

Similarly, Zhu et al. [163] prepared MWCNTs-Co/a-C: H films on the surface of silicon wafers by composite electrodeposition with a static contact angle of 158.1° and a rolling angle of 2.98°. The anti-corrosion efficiency of the prepared coating in 3.5 % NaCl solution reached 98.02 %, and the sandpaper wear test also proved that it had good wear resistance.

3.3.2.3. Other composite superhydrophobic coatings. Polytetrafluor oethylene (PTFE) has the lowest surface energy of all polymers and has a low coefficient of friction, which has been widely used in the manufacture of self-lubricating materials. Besides, it also has good heat resistance as well as chemical stability [164]. Therefore, if PTFE particles are co-deposited directly on the surface of the coating, a good hydrophobic effect can be achieved without modification, and its chemical inertia can also enhance the anti-corrosion effect. Daniel et al. [165] added PTFE particles and saccharin (grain refiner) to the watt bath and fabricated superhydrophobic Ni-PTFE composite coating on copper surface by electrodeposition at the current density of 100 mA/cm^2 for 30 min. With the increase of PTFE content in the composite deposition layer, the hydrophobicity increased gradually and the WCA of the coating surface reached the maximum value of 152°. SEM observation found that the average sizes of PTFE particles in the

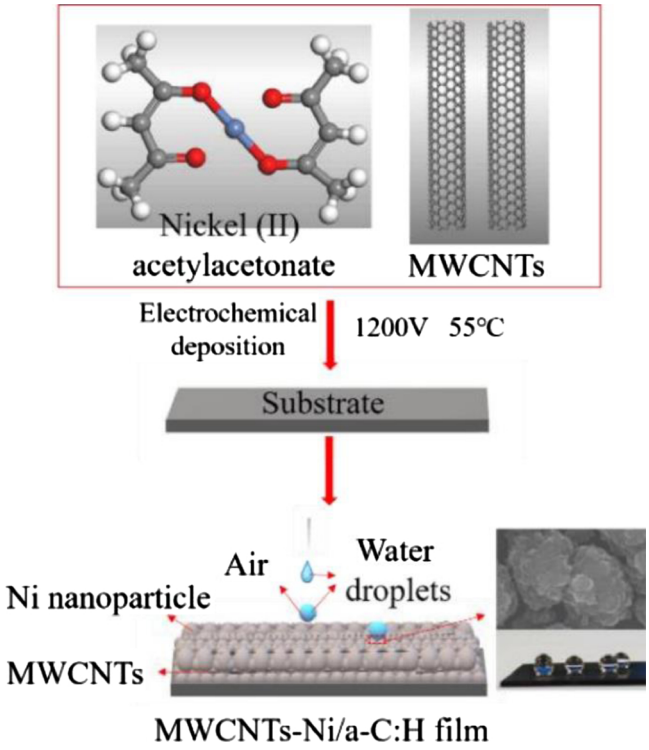

Fig. 8. Schematic of the preparation process of superhydrophobic MWCNTs-Ni/a-C:H film [162].

coating were 8 μm and 0.6 μm, and such dual-scale structure was undoubtedly beneficial to the realization of superhydrophobic effect. The hardness test showed that too high PTFE content would lead to the decrease of the hardness of the coating, while in the subsequent wear resistance test [38], it was found that the decrease in hardness would not reduce its wear resistance because the PTFE particles were deposited in the Ni coating by embedding. Therefore, PTFE can provide continuous hydrophobicity in the wear process. Compared with other spray superhydrophobic coatings, the Ni-PTFE coatings prepared by electrodeposition showed better mechanical stability.

Composite electrodeposition has great flexibility, in which there may not be only one kind of particle, but a variety of particles can be added to the deposition phase, so the composite coating has the advantage of multiple particles. Zhou et al. [166] prepared Ni/WC/WS_2 composite superhydrophobic coating on the surface of low carbon steel by co-deposition of WC and WS_2. The WCA was 170°, and the SA was close to 0°. WS_2 itself is a kind of self-lubricating material, which can effectively reduce the friction coefficient of the coating surface, while WC has a high melting point, high hardness, and good chemical stability. Based on the above two points, the prepared composite coating had excellent superhydrophobicity, anti-corrosion effect, wear resistance, and durability.

Also, other successful cases of superhydrophobic composite coatings prepared by electrodeposition in the past five years are listed in Table 2. To sum up, composite electrodeposition makes up for the shortcomings of common metal electrodeposition and non-metallic electrodeposition. By adding suitable particles to the electrolyte solution, the secondary surface modification can be avoided, and the wear resistance and stability of the coating can be improved so that the coating can provide a more significant and durable anti-corrosion effect for the substrate. At the same time, composite electrodeposition also provides an idea for the preparation of multi-functional composite superhydrophobic coatings.

4. Process parameters of electrodeposition

In the electrodeposition process, many factors will affect the composition and surface morphology of the deposited coating, and then affect the hydrophobicity and anti-corrosion efficiency, among which the bath composition, electrodeposition time and current density are the three main factors.

4.1. Crystal modifiers

The electrolyte solution used in the electrodeposition process is generally composed of the following components: the main salt, which provides salt ions deposited on the cathode; the conductive salt, which enhances the conductivity of the solution; the buffer, used to stabilize the pH of the solution, especially the pH near the cathode; the anode activator, to eliminate or reduce the anodic polarization and ensure the normal dissolution of the anode; additives, small additions of which have a significant effect on the coating, such as brightener, leveling agent, wetting agent, etc. The effects of these components on the properties of the coating have been well summarized in the previous literature about the electroplating process, which will not be introduced too much in this paper. Coating morphology is an important factor affecting the wettability, and in recent years, in the practice of electrodeposition preparation of superhydrophobic coatings, it is found that some reagents can regulate the crystal growth process and induce the formation of micro-nano dual-scale structures, thus regulating the coatings morphology. It is beneficial to the realization of superhydrophobicity, and these substances are called crystal modifiers.

Soleimangoli et al. [173] added different proportions of ammonium chloride crystallization modifier to the electrolyte composed of nickel chloride, zinc chloride, and boric acid, and prepared a superhydrophobic Ni-Zn coating on the surface of copper sheet by two-step electrodeposition. It was found that the surface of the coating was polyhedral when ammonium chloride was not added, and with the addition of ammonium chloride, the morphology of the coating changed from polyhedral-shape structure to micro/nano-conical structure. The roughness increased gradually, and the best hydrophobic effect was achieved when the content of ammonium chloride reached 400 g/L, and the WCA reached 154.8° without any surface modification. Compared with the coating prepared without NH_4Cl, the corrosion current density of this coating was three orders of magnitude lower, so a better anti-corrosion effect was achieved.

Similarly, Hashemzadeh et al. [174] prepared the superhydrophobic Ni coating on the copper surface with the mixed solution of $NiCl_2$, H_3BO_3, and a certain amount of NH_4Cl as electrolyte. The modification effect of NH_4Cl on crystallization was also found in the preparation process, which transformed the single-stage micro-cone into hierarchical micro/nano-cone structure and induced a superhydrophobic effect. They further explored the role of NH_4Cl in this process by cyclic voltammetry and electrochemical impedance spectroscopy. They found that the addition of NH_4Cl could increase the activation energy of nucleation, while reducing the solution resistance and increasing the charge transfer resistance of the system. NH_4Cl is a strong complexing agent [175], and NH_4^+ formed when dissolved in water will react with Ni^{2+} as follows: $Ni^{2+}+xNH_4^+ \rightarrow [Ni(NH_3)_X]^{2+} + xH^+$. Therefore, the existing form of Ni^{2+} in the solution has changed from $[Ni(OH)]^+$ and $[Ni(Cl)]^+$ to $[Ni(NH_3)x]^{2+}$ partly. Metal ions need to undergo the dissociation process of complexes before being reduced and deposited, and as shown in Table 3 and 4, the dissociation energy of most ammonium complexes is higher than that of the other two, which makes the electrode reaction more difficult, thus inhibiting the nucleation process on the surface of the cathode and affecting the morphology of the coating.

of nickel complexes at 298 K [176,177]

The effect of NH_4Cl on the coating morphology can also be explained by the screw dislocation growth theory. It is generally believed that in the early stages of crystal growth, atoms are deposited in a layer growth mode. However, as the atoms continue to accumulate, internal stress is accumulated in the lattice due to the uneven distribution of impurities or thermal stress, resulting in the relative shear displacement of the lattice and the formation of dislocations. The appearance of dislocations provides a step source that will never disappear at the interface of the crystal. With the progress of growth, the steps will be spirally distributed around the dislocation, making the crystal grow in a spiral shape. The step distance of screw dislocation can be determined by Eq. (6) [178,179]:

$$d = 19\rho_c = \frac{19V_m\gamma}{kTLn(1+\sigma)} \tag{6}$$

where σ is the relative supersaturation of the solution at the growth interface, which is determined by Eq. (7):

$$\sigma = \frac{a}{a_*} - 1 \tag{7}$$

where a and a_* represent the activity of solute in supersaturated and saturated solutions, respectively. It can be found that the greater the supersaturation, the smaller the step distance. It has been analyzed above that the addition of crystal modifiers makes the discharge intermediates more complex, not just hydrolysates and chlorides [174], which increases the supersaturation of the solution and reduces the step distance, and thus reduces the crystal size and resulting in a micro-nano dual-scale structure.

Rahimi et al. [74,180] found that H_3BO_3 was also an effective crystal modifier, which strengthened the growth mechanism of spiral dislocations by adsorbing on one side of the crystal in the nickel ion electrolyte and then limiting the growth of the crystal on the high energy plane. Hashemzadeh et al. [174] also explained that the crystal modifier could change the preferred orientation of the crystal, which affected the morphology of the surface and then influenced the wettability and anti-corrosion performance of the coating.

In addition to NH_4Cl and H_3BO_3, ethylenediamine is also added to the electrolyte solution as a crystallization modifier to adjust the microstructure of the coating surface [119,181]. However, in the field of superhydrophobic coating preparation, there are still few crystal modifiers reported at present, and the mechanism of regulating the micro-morphology remains to be further studied.

4.2. Current density

Many researchers studied the effect of current density on coating morphology and wettability [127,182]. It was found that the crystal size deposited on the surface of the coating was larger at lower current density, and the crystal size decreased with the increase of current density, as shown in Fig. 9 (a), (b). As the current density continued to increase, the micro-nano dual-scale structure appeared on the surface of the coating, as shown in Fig. 9 (c), (d). And the hydrophobicity increased gradually. The above phenomenon is due to the grain refinement caused by the increase of current density in a certain range. With the increase of current density, the cathodic overpotential increases and provides an additional driving force for nucleation, so the rate of nucleation on the cathode is greater than that of crystal growth, and the crystal size decreases because the crystal nucleus cannot grow in time [183]. However, when the current density reaches the diffusion-limited value, the current density is large enough that the electrodeposition process is controlled by the material diffusion process. Only part of the ions can reach the surface of the cathode in time and be deposited by discharge, so only part of the crystals can continue to grow while other crystals are passivated, resulting in the appearance of micro-nano dual-scale structure on the surface.

Nevertheless, the superhydrophobicity, and anti-corrosion performance of the coating are not always positively related to the current density. Liu et al. [114] prepared superhydrophobic coating on the steel

Table 3
Examples of superhydrophobic composite coatings fabricated by electrodeposition.

Matrix	Coating	Electrolyte composition	Process conditions	WCA	SA	ref
316 L steel	TiO_2/TMPSi	TiO_2 + TMPSi + Iodine + acetylacetone	5 V (45 s) + increase the voltage at 1 V/s until 30 V in 45 s–70s	168°	3.1°	[34]
Copper	Ni/TiO_2/TMPSi	Plating solution: $NiCl_2$ + H_3BO_3 + $NiSO_4$ + SDS + TiO_2 Modification : TMPSi	80.7 A/dm^2(19.17 min), 50.5 °C + Surface modification	151.6°	6.2°	[37]
Ti_6Al_4V	Zn/ZnO/TiO_2	Etching liquid: HCl Plating solution: $Zn(Ac)_2$ + KCl + HCl	Chemical etching + −1.5 V (10 min) + annealed (90 °C, 60 min)	160°	< 1°	[167]
mild steel	Ni/WS_2	$NiSO_4$ + $NiCl_2$ + H_3BO_3 + CTAB + WS_2 + Saccharin	4 A/dm^2 (20 min), 40 °C	158.3°	7.7°	[168]
mild steel	Ni-P/WS_2	$NiSO_4$ + H_3BO_3 + NaH_2PO_2, + HOC(COOH)($CH_2COOH)_2$ + $NiCl_2$ + WS_2 + CTAB	2.5 A/dm^2 (45 min), 60 °C	157°	—	[169]
Stainless steel	Cu/MoS_2	$CuSO_4$ + H_2SO_4 + MoS_2 + CTAB + thiourea	50 mA/cm^2(2 min)	158.2°	1.8°	[170]
Carbon steel	Ni/WC	$NiSO_4$ + $NiCl_2$ + H_3BO_3 + CTAB + WC	6 A/dm^2 (30 min), 40 °C	164.3°	0°	[171]
Copper	Ni/PTFE	$NiSO_4$ + $NiCl_2$ + H_3BO_3 + PTFE particles	100 mA/cm^2(15 min), 60 °C	≈155°	—	[172]

surface and found that when the current density was low, the crystal structure deposited on the substrate was sparse and uneven, and the nanostructure could not grow. With the increase of current density, the bud structure began to grow and gradually formed a micro-nano dual-scale structure, which made the hydrophobicity increase continuously. However, when the current density continued to increase, the continuous growth of the crystals led to the disappearance of the nanostructure, as a result, the crystal structure changes into a single micron structure.The single micron structure is not conducive and hinder the realization of the superhydrophobic effect. Liu et al. [123] found that there was an optimal current density when preparing ceria superhydrophobic coating on the surface of magnesium alloy. Increasing the current density would increase the number of cracks and widen the cracks, which would adversely affect the anti-corrosion performance. Therefore, the optimal hydrophobicity and corrosion resistance depends on a reasonable current density.

4.3. Electrodeposition time

Regarding the effect of electrodeposition time on the hydrophobic performance of the coating, there is an optimal value of deposition time. Before this critical point, the hydrophobicity increases with the increase of deposition time, while beyond the critical point, the increase of deposition time will lead to the decrease of the hydrophobic effect.

Superhydrophobicity depends on the appropriate surface morphology, and the effect of deposition time on the wettability is exactly achieved by affecting the coating morphology. When Li et al. [36] prepared the superhydrophobic zinc coating on the steel surface by the two-step electrodeposition method, they found that the WCA gradually increased as the secondary deposition time increased from 1 min to 3 min, and SEM observation showed that the surface morphology changed from flat to full of texture, and meanwhile, the roughness increased continuously. As the deposition time continued to increase, the WCA did not increase anymore but decreased, and the results of SEM showed that the surface became relatively flat again without lots of texture structures, and the roughness also decreased.

Simultaneously, if the deposition time is too short, the coating is easy to crack and warp because of its-small thickness. Liu et al. [123] found that the coating surface was full of cracks and bends when the deposition time was only 5 min, as shown in Fig. 10 (a1). Even after surface modification, the adhesion between the droplets and the surface was still extensive, so a good anticorrosive effect could not be achieved. When the deposition time was gradually increased to 60 min, the thickness of the coating increased, and more and more nanosheet structures were deposited on the surface of the coating. The cracks disappeared, and the coating surface became denser, as shown in Fig. 10 (b1), (c1), and of course the superhydrophobic and anti-corrosion effect was strengthened. In summary, the anticorrosive superhydrophobic coating is different from other anticorrosive coatings, whose anticorrosive function is realized by superhydrophobicity related to surface morphology, so the requirement of deposition time is more stringent.

5. Development of electrodeposition technology

Traditional electrodeposition technology has been widely used in the fabrication of superhydrophobic coatings for corrosion protection, but with the deepening of research, electrodeposition technology has been developed and shows unique advantages.

5.1. Pulse electrodeposition

Pulse electrodeposition is a processing technology in which the current is turned on and off according to a specified pattern. Compared with the traditional continuous DC electrodeposition, many characteristics of pulse electrodeposition make it especially suitable for the preparation of superhydrophobic coatings [184,185]. During the current conduction period, the metal ions near the cathode are continuously reduced and deposited, so that the ion concentration decreases rapidly. While during the current turn-off period, the ion reduction process stops, and the metal ions diffuse from the bulk solution to replenish the ion concentration near the cathode. Thus, the thickness of the diffusion layer reduces, and the concentration polarization decreases as well, so that the upper limit of the current density is increased. In electrodeposition, the two-dimensional nucleation rate H, the critical radius of the crystal nucleus r_e and the cathodic

Table 4
Thermodynamic equilibrium constants for the formation.

Particle	$[Ni(Cl)]^+$	$[Ni(OH)]^+$	$[Ni(NH_3)]^{2+}$	$[Ni(NH_3)_2]^{2+}$	$[Ni(NH_3)_3]^{2+}$	$[Ni(NH_3)_4]^{2+}$	$[Ni(NH_3)_5]^{2+}$	$[Ni(NH_3)_6]^{2+}$
Log K	−1.29	3.58	2.81	5.08	6.85	8.12	8.93	9.08

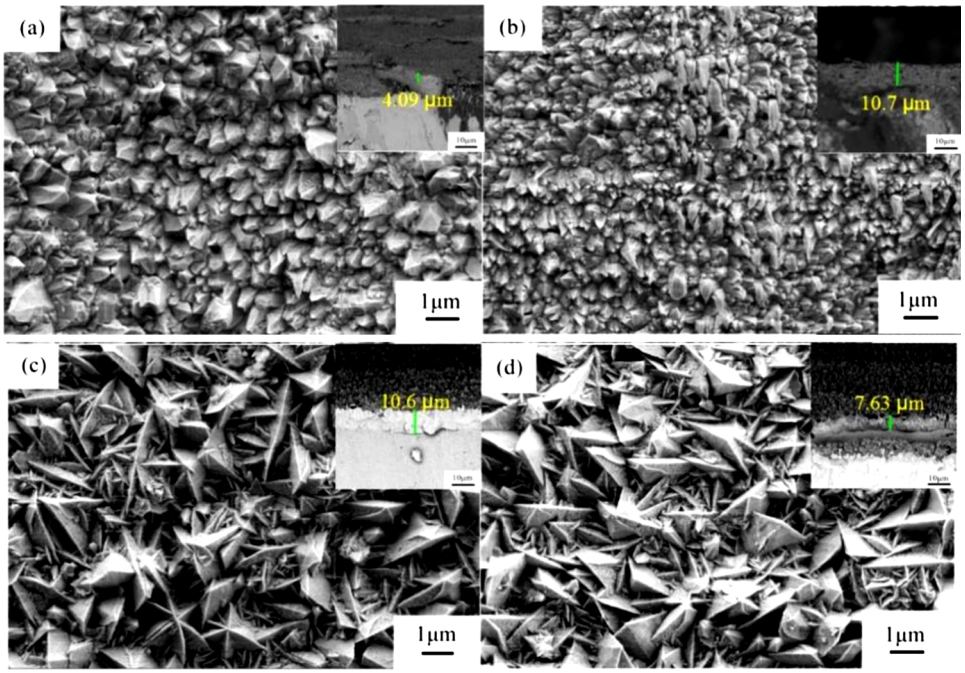

Fig. 9. SEM images of nickel coatings deposited with increasing current density [182].

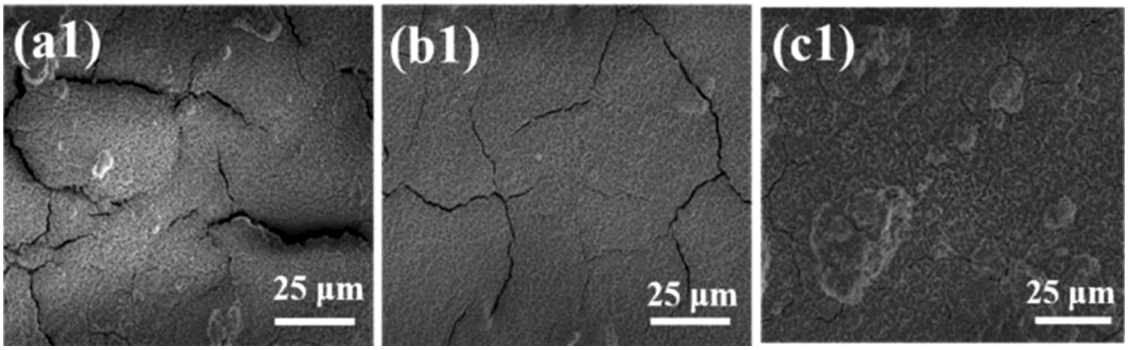

Fig. 10. SEM images of coatings deposited with increasing deposition time [123].

overpotential η satisfy the following relations, respectively [186]:

$$H = k_1 \exp\left(-\frac{bs\varepsilon^2}{zeKT\eta}\right) \tag{8}$$

$$r_e = \frac{\pi h^3 E}{6ze\eta} \tag{9}$$

By analyzing Eq. (8) and Eq. (9), it can be proved that the nucleation rate H increases with the increase of the cathodic overpotential η, while the critical radius of the crystal nucleus r_e decreases with the increase of the cathodic overpotential η. Therefore, the cathodic overpotential increases under the higher current density, which promotes the nucleation process. At the same time, the epitaxial growth of the crystal is hindered during the current turn-off period, so the grain coarsening is avoided. Such characteristic of pulse electrodeposition is particularly conducive to the growth of micron and nano-scale structures, and as mentioned above, the micro-nano dual-scale structure of the coating surface is the key to the realization of superhydrophobicity. In addition, pulse electrodeposition can also reduce the hydrogen evolution reaction of the cathode and improve the quality of the coating.

Besides, compared with ordinary DC electrodeposition, pulse electrodeposition has more adjustable parameters including waveform, period, frequency, duty cycle, current density, and deposition time, all of which will affect the performance of the coating, so the morphology of the coating can be better controlled. The parameters of pulse electrodeposition satisfy the following relations:

$$T = T_{on} + T_{off} \tag{10}$$

$$f = \frac{1}{T} \tag{11}$$

$$\gamma = \frac{T_{on}}{T} = \frac{T_{on}}{T_{on} + T_{off}} \tag{12}$$

$$I_p = \frac{I_m}{\gamma} \tag{13}$$

where T, T_{on} and T_{off} are the period, pulse-on and pulse-off time, respectively; f and γ are the frequency and the duty cycle; I_p and I_m are the peak and average current density.

Chen et al. [187] prepared a superhydrophobic nickel coating on the copper substrate by pulse electrodeposition. The effects of peak current density, pulse-on time, and duty cycle on the morphology and wettability of the coating were investigated systematically. They found that with the increase of the peak current density, the density of the nickel cone increased, and the size of crystals decreased. While with the increase of the duty cycle, the roughness of the side wall of the nickel cone increased, and the secondary growth of nanocrystals appeared. The effect of pulse-on time on the morphology of the coating was

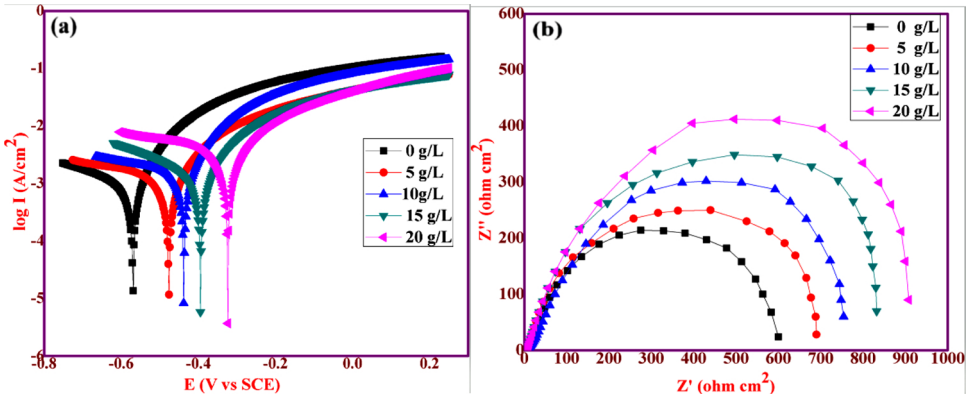

Fig. 11. (a) Potentiodynamic polarization curves and (b) Nyquist plot of Ni–W alloy matrix and the Ni–W/PTFE coatings with different concentrations of PTFE particles [188].

similar to that of the duty cycle. More specifically, sharper cones covered with irregular secondary nuclei were observed with the extension of pulse-on time. As analyzed above, the effects of these parameters on the morphology of the coating are realized by affecting the cathodic overpotential and ion mass transfer process.

Sangeetha et al. [188] prepared a superhydrophobic Ni-W/PTFE composite coating on the surface of carbon steel by pulse electrodeposition, which not only achieved the superhydrophobic effect, but also obtained self-lubricating properties. Fig. 11 shows the results of potentiodynamic polarization curves and electrochemical impedance spectroscopy of typical Ni-W alloy coating and superhydrophobic Ni-W/PTFE coating. It can be seen that the hydrophobic coating with different concentrations of PTFE particles has lower corrosion current density, more positive corrosion potential, and larger arc radius than ordinary Ni-W alloy coating, so the Ni-W/PTFE superhydrophobic coating by pulse electrodeposition had better anti-corrosion performance.

5.2. Jet electrodeposition

Jet electrodeposition technology refers to that the electrolyte is jetted onto the workpiece at a high speed while a certain voltage is applied between the cathode (workpiece) and the anode (nozzle). There is current passing through the jet coverage area where electrodeposition occurs, while substances cannot be deposited in areas where there is no electric current. Therefore, compared with traditional electrodeposition techniques, jet electrodeposition has many unique advantages [189,190].

First of all, jet electrodeposition is selective. Through the relative movement of anode nozzle and cathode, metal or other substances can be selectively deposited in the desired area, which can not only save raw materials, but also make it simple to implement electrodeposition in many complex parts. Secondly, the mass transfer of the high-speed jet to the workpiece surface is strong, which greatly reduces the diffusion layer on the cathode surface, thus creating conditions for increasing the limit of current density. Similar to pulse electrodeposition, the high current density increases the cathodic overpotential, which can effectively refine the grains and induce the appearance of micro-nano scale to improve hydrophobicity. What's more, the higher current density can also effectively improve deposition efficiency. Finally, the higher jet velocity greatly reduces the adhesion of hydrogen bubbles on the surface of the cathode, thus reducing the defects such as hydrogen embrittlement, pinholes, pitting, and so on.

Shen et al. [75] sprayed the electrolyte solution containing nickel ions from the nozzle to the graphite substrate surface at a speed of 4 L/min, and successfully prepared the superhydrophobic nickel coating by jet electrodeposition. SEM observation showed that the surface of the coating was covered with cauliflower-like clusters, which was crucial to superhydrophobicity. The maximum WCA reached 155.4°, and the SA was as low as 6.5°. The superhydrophobic effect of the coating was not lost after being exposed to air for 6 months and stored at 200 °C for 4 h, which proved that the coating had good stability.

5.3. Magnetic field-induced electrodeposition

Many literatures have proved that the introduction of magnetic field in the process of electrodeposition can significantly affect the composition and morphology of the coating. Thiemig et al. [191] studied the electrodeposition process of nano-Co particles and magnetite particles in nickel-based metals in a static magnetic field. It was found that the magnetic field perpendicular to the cathode surface could significantly increase the deposition amount of nanoparticles in the nickel base, while the parallel magnetic field would reduce the co-deposition amount. Bund et al. [192] observed the electrodeposition process of nickel in the magnetic field (perpendicular to the current line) and found that the limiting current density of the cathode increased and the crystal size decreased after applying the magnetic field, which was consistent with the reference [193].

The influence of the magnetic field on the electrodeposition process comes from two aspects. On the one hand, it is the result of the magnetohydrodynamic (MHD) effect, that is, the Lorentz force acts on the moving charge perpendicular to the magnetic field, so the mass transfer rate in the electrolyte solution must be affected by the magnetic field. It has been proposed that the effect of the magnetic field on the material transport is equivalent to gently stirring [194]. On the other hand, in composite electrodeposition, if the co-deposited particles are ferromagnetic, they will inevitably flow to the area with high magnetic flux density. Based on the above two points, the application of the magnetic field in the process of electrodeposition is helpful in controlling the morphology of the coating.

Shen et al. [59] prepared Ni/Nip anti-corrosive superhydrophobic coating on the surface of the copper sheet by magnetic field-induced scanning electrodeposition. As shown in Fig. 12, they added ferromagnetic nano-nickel particles Nip with a diameter of about 500 nm into the traditional plating solution and generated a parallel uniform magnetic field in the processing area by applying a constant DC current to the electromagnet. The synergistic effect of magnetic field and electrodeposition made the cathode surface form a uniform distribution of micron-nanometer layered structure, while the composite coating without magnetic field had a disorderly particle distribution and uneven particle size. After five days of exposure in the air, the coating changed from a hydrophilic state to a superhydrophobic state, and the maximum contact angle could reach 155.4° when the magnetic field strength was 120 m T. The change in wettability may be attributed to the oxidation of nickel exposed to the air to produce hydrophobic NiO [195], or the reduction of surface energy due to the contamination of

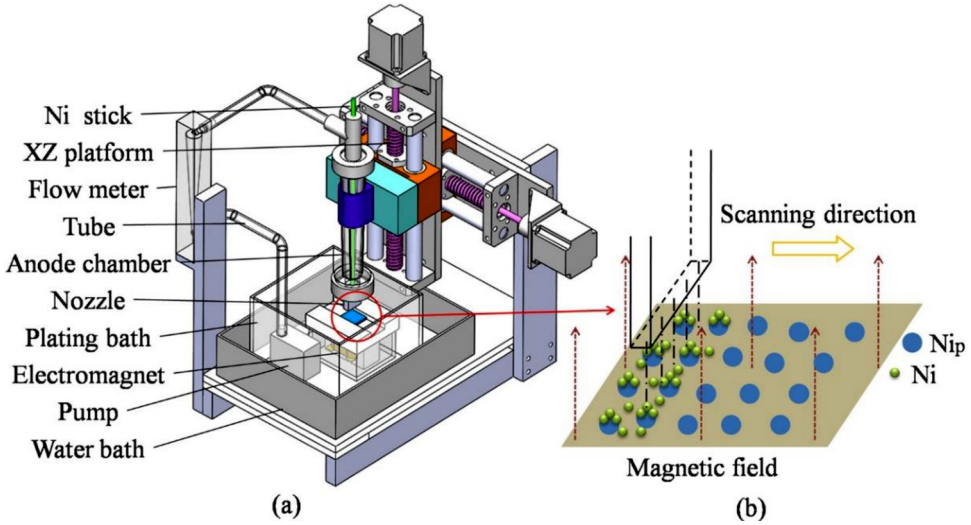

Fig. 12. Schematic diagram of magnetic field induced electrodeposition technique [59].

the coating surface by hydrocarbons in the air [196]. The potentiodynamic polarization curve of the coating was measured in 3.5 % NaCl solution, and the calculated corrosion potential and corrosion current density were only -0.237 V and 0.06 μA/cm^2, which showed an excellent anticorrosive effect. However, the mechanical strength and durability of the coating have not been reported.

5.4. Ultrasound-assisted electrodeposition

Ultrasound is an acoustic wave with a frequency higher than 20,000 Hz. Research has found that during electrodeposition, ultrasound can not only improve the dispersion of nanoparticles in the plating solution, but also significantly change the morphology of the coating [197]. The effect of ultrasonic on the electrodeposition process is due to the ultrasonic cavitation. As shown in Fig. 13, ultrasound propagates in the liquid medium by performing a series of periodic cycles of compression (positive pressure) and expansion (negative pressure). During the negative pressure cycle, the intermolecular "expanding" force is greater than the "attraction" force, resulting in tiny bubbles in the solution. Then the bubbles continue to gain energy and expand in volume, and finally, the bubbles collapse and release a large amount of heat, shock waves, and jets at the moment of destruction, which has a physical and chemical impact on the electrodeposition process [198].

It is generally believed that ultrasonic cavitation will have the following three effects on the electrodeposition process. The first is the strengthening effect on the deposition process. The strong stirring effect of the ultrasonic cavitation micro-jet on the solution can strengthen the transportation of ions, reduce the thickness and the concentration gradient of a diffusion layer, thereby reducing the concentration polarization and accelerate the electrodeposition process. The second is to refine the grains. Ultrasonic cavitation can produce local high temperature and high pressure, at the same time, it can cause the adjacent

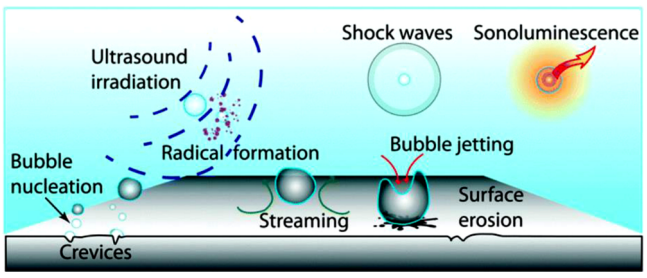

Fig. 13. Schematic diagram of ultrasonic cavitation effect [198].

local instantaneous low temperature, prevent grain growth, reduce the critical nucleation radius and improve the nucleation rate. The third is the stirring and dispersion of nanoparticles. Ultrasonic cavitation can crush the agglomerated nanoparticles and make the nanoparticles uniformly distribute in the electrolyte.

In preparing superhydrophobic coatings, especially composite coatings by electrodeposition, many researchers have used ultrasonic waves to obtain plating solutions with good dispersibility [166,199]. Tudela et al. [200] studied the electrodeposition process of WS_2 nanoparticles in a nickel matrix under the action of ultrasound and found that the ultrasound could significantly increase the number of nanoparticles deposited in the coating. At the same time, the distribution of nanoparticles in the coating was more uniform and the grain size of the coating was obviously refined. The hardness of the coating was also improved. Li et al. [50] prepared Ni-Cu/TiN composite coating on copper substrate by ultrasound-assisted electrodeposition. It was found that the introduction of the ultrasonic wave improved the comprehensive properties of the composite coating, especially its anti-corrosion performance. In a word, ultrasonic cavitation can refine the grain size and control the morphology of coatings, which makes it have great potential in the preparation of superhydrophobic coatings by electrodeposition.

All in all, these new developments of electrodeposition technology are still seldom used in the preparation of anticorrosive superhydrophobic coatings up to now. However, existing research has already demonstrated their great advantages in regulating coating morphology, increasing deposition rate, and so on. Therefore, increasing research on these new developments will facilitate the true industrial preparation and application of anticorrosive superhydrophobic coatings.

6. Other applications of electrodeposited layers

6.1. Anti-icing and self-cleaning

In addition to anti-corrosion, electrodeposited layers with special wettability are also used in other fields. Anti-icing superhydrophobic coatings have been a research hotspot in recent years, because icing has caused serious harm to the glass of buildings, the normal operation of solar panels, the safety of aircraft, and other aspects [201]. On the one hand, the strong water repellency of the superhydrophobic surface enables water droplets to roll off the matrix surface before freezing at subzero temperature; On the other hand, the "air pockets" formed among the micro-nano structures act as a thermal insulation layer,

which can prevent heat conduction during icing and reduce ice adhesion [202]. Wang et al. [203] found that ice and frost would not adhere to the penguin's body even in extremely cold conditions because their feathers were covered with micro-nano hierarchical structures. Cheng et al. [204] prepared superhydrophobic $CuZn_5$ and $AuZn_3$ surface on the copper surface by combining electrodeposition at a constant voltage, electroless chemical deposition, and annealing treatment. The WCA was as high as 170°, and the SA was close to 0°. When the temperature reached −16 °C, the water droplets on the untreated copper surface had begun to freeze, while the droplets on the superhydrophobic surface were still in the liquid state.

Except for electrochemical deposition, other methods have also been used to prepare anti-icing superhydrophobic coatings. Zheng et al. [205] prepared superhydrophobic coatings on aluminum by anodizing at constant voltage followed by surface modification with FAS (1*H*,1*H*,2*H*,2*H*-perfluorodecyltriethoxysilane). Compared with the bare Al surface, the water droplets on the superhydrophobic surface began to freeze at a lower temperature, and it took a longer time to reach the fully frozen state. In other words, the possibility of freezing on superhydrophobic surfaces is greatly reduced. Besides, references [206–208] also reported anti-icing superhydrophobic coatings prepared by other technologies.

Anti-pollution is another basic function that a superhydrophobic surface can achieve. Water droplets can easily roll off the hydrophobic surface, so dust and other pollutants can be carried to achieve the purpose of self-cleaning, just like lotus leaves and flowers [209]. Liu et al. [114] prepared superhydrophobic Cu-Ni coatings on the surface of 316 l stainless steel by electrodeposition with WCA and SA of 161.27° and 7.8° respectively. Fig.14 shows the self-cleaning process of bare steel substrate and superhydrophobic coating surface. Obviously, water droplets accumulated and spread on the surface of the steel substrate while rolled off and took away contaminants as soon as they touched the superhydrophobic surface.

6.2. Electrodeposited catalysts for water splitting

With the development of economy and society, people's demand for energy is increasing. However, the storage of non-renewable energy sources such as oil, natural gas, and coal is gradually decreasing, and their combustion has also caused serious environmental pollution [210]. Hydrogen has the advantages of cleanliness, high calorific value, and regeneration, which makes it a good alternative energy source. Up to now, commercial hydrogen production is mainly through fossil fuel steam reforming [211], which also causes energy waste and environmental pollution. Electrocatalytic and photocatalytic water splitting to produce hydrogen are very potential hydrogen production methods [212,213]. Therefore, the preparation of high-efficiency electrocatalysts and photocatalysts is the key to the realization of hydrogen production by water splitting.

Among all catalyst preparation technologies, electrodeposition has been widely used in recent years due to its convenient operation and easy control [214]. Platinum-based and other precious metal catalysts have been proved to have good hydrogen and oxygen production performances, while their applications are limited by the high price and poor stability [215]. In consequence, non-precious metal materials such as transition metal-based catalysts have attracted people's attention. For example, Xu et al. [214] prepared $Ni(OH)_2$ nanosheets containing NiS and Ni_2P nanoparticles on a foamed nickel substrate by electrodeposition. The reference [216] reported an electrodeposition process for preparing CoNi alloy nanosheet arrays on a copper foam substrate. These successful practices have achieved a good catalytic effect.

As we all know, almost all catalytic reactions are carried out on the surface of the catalyst. Therefore, the surface state of the electrodeposited layers, such as surface composition, structure, morphology, defects, etc., will strongly affect the catalytic activity [213]. Previous studies have shown that the catalytic performance is related not only to the active sites of the catalyst, but also to the adsorption of the reactants and products on the catalyst surface. As a result, the appropriate wettability promotes the adsorption and transfer of the reactants or products on the catalyst surface, thus enhancing the reaction activity [217,218].

Contrary to hydrophobicity, studies have shown that increasing hydrophilicity can effectively improve the catalytic activity of water splitting. Li et al. [217] prepared a NiFe/NiFe: Pi electrocatalyst composed of NiFe hydroxide and NiFe phosphate based on electrodeposition technology. They first prepared a layer of NiFe hydroxide on carbon fiber paper by electrodeposition, and then converted part of NiFe hydroxide into phosphide by reacting with phosphorus vapor, as shown in Fig.15. Through testing, the NiFe hydroxide electrodeposited layer was hydrophobic with a contact angle of 129 ± 5°, while after phosphorylation, the contact angle quickly dropped to 44 ± 3°, that is, the layer became hydrophilic. An excellent electrocatalyst for water splitting should have a smaller overpotential in the electrochemical reaction to reduce the energy consumption, which is an important indicator for evaluating the electrocatalytic performance of materials. The overpotential required for delivering a current density of 10 mA/cm^2 for the hydrophilic NiFe/NiFe: Pi layer was merely 290 mV, in contrast, it was 320 mV for the hydrophobic NiFe hydroxide. In other words, the enhancement of hydrophilicity makes it easier for the solution to adsorb on the surface of the catalyst, thus achieving higher catalytic activity.

Kutyła et al. [219] prepared a Co-Ni-Rh ternary electrocatalyst on the copper surface by potentiostatic electrodeposition and studied its hydrogen evolution activity in 6 M KOH solution through electrochemical tests. The overpotentials of the bare copper substrate, Cu/Co-Rh, Cu/Ni-Rh, and Cu/Co-Ni-Rh electrodes at 100 mA/cm^2 were 466,

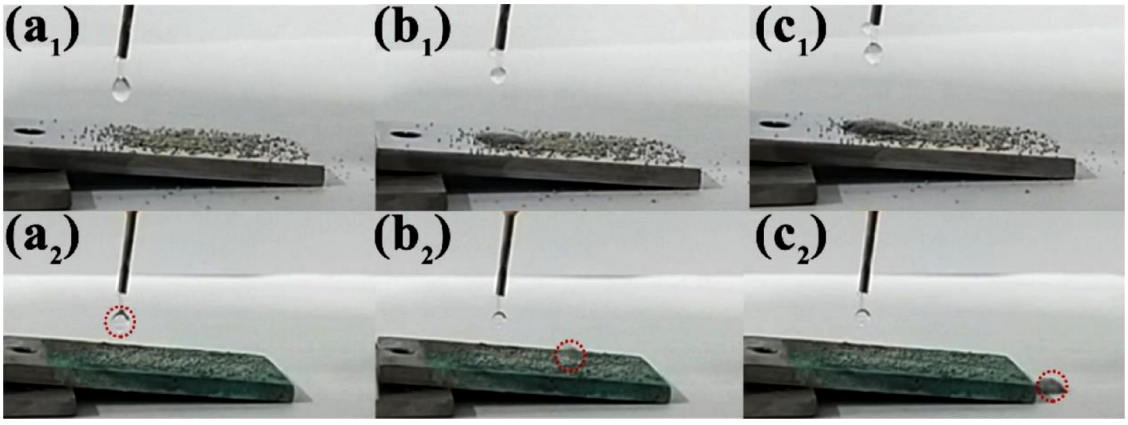

Fig. 14. Self-cleaning process on the different samples: (a1), (b1), (c1) steel substrate; (a2), (b2), (c2) superhydrophobic Cu-Ni coating [114].

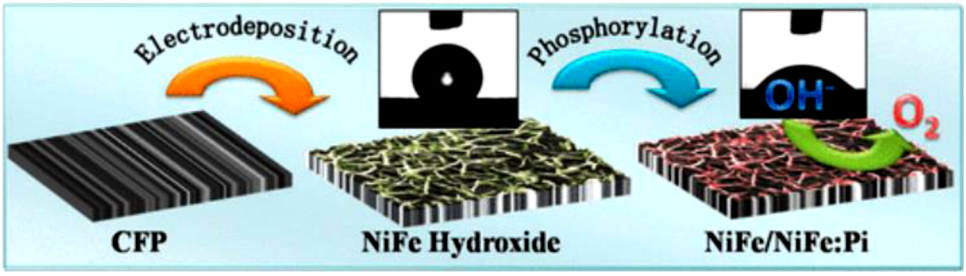

Fig. 15. Schematics of NiFe/NiFe:Pi 3D-hierarchical nanostructures fabricated in the first step by electrodeposition followed by the second-step phosphorylation process [217].

214, 102 and 76 mV, respectively, indicating that the same hydrogen volume could be obtained at a lower overpotential on the ternary alloy electrode. The increase in catalytic activity was due to the increase in electrochemically active area [220] because regular porous structure could be observed on the surface of the Co-Ni-Rh ternary electrodeposited layer, which proved the effect of surface state on catalytic performance again.

7. Challenges and outlooks

The electrodeposition method has been successfully used to prepare superhydrophobic coatings. However, most superhydrophobic coatings are only prepared in the laboratory and have not been applied on a large scale, which should be attributed to the following reasons:

(1) The prepared superhydrophobic coating still has relatively poor durability and stability. On the one hand, the coating is easy to fall off in the use process due to the poor adhesion between the coating and the substrate. On the other hand, the surface structure of the coating will be destroyed under a small impact because of the fragility of the micro-nano structure. Moreover, many preparation methods proposed now rely on the use of low surface energy materials to modify the surface, and once this layer of material attached to the surface falls off, the superhydrophobic property will be lost. And as a result, the coating can not provide long-term corrosion resistance. For instance, Huang et al. [221] prepared superhydrophobic coatings on different substrates using modified TiO2 and PDMS, and then tested the durability of the coatings in pH = 1 HCl, pH = 14 NaOH, and pH = 5 CH3COOH solutions. The results showed that the static contact angle had been reduced to below 150° after the coating was immersed in the strong acid solution for only 5 h or in the strong alkaline solution for 3 h, that is, the superhydrophobicity had disappeared. In the weak acid solution, the superhydrophobicity of the coating was maintained for 6 h, but it is far from meeting the requirements of practical application. Tan et al. [222] prepared a superhydrophobic coating on the surface of stainless steel and tested its durability in 1 mol/L sodium hydroxide, 1 mol/L sulfuric acid and 3.5 wt.% salt solution. After a 20 d immersion experiment, the WCA of the coating decreased slightly while the SA sharply increased to more than 15°, and the superhydrophobicity was greatly damaged.
(2) Condensation problem. The superhydrophobic coating is water hydrophobic, but it loses its resistance to water vapor, which can be attached to the surface of the hydrophobic coating. When it is below the dew point, the water vapor condenses and fills in the micro-nano structures of the coating, sot that the superhydrophobic effect of the coating is lost.
(3) Emulsifier/oil wetting problem. Due to the serious corrosion problem, the petroleum industry is a huge potential application field of superhydrophobic anticorrosive coatings. However, the presence of oil and emulsifier can significantly reduce the surface tension of water droplets, resulting in the loss of superhydrophobicity. Therefore, preparation of both oleophobic and hydrophobic coatings is an important topic in the future.
(4) Preparation process problem. Although many successful cases of preparing superhydrophobic coatings by electrodeposition have been reported in many literatures, it can be found that there are great differences in bath composition, current density, deposition time and other process conditions. Even if the composition of the coating is the same, the process used is different. Therefore, there is still a lack of a set of authoritative and complete technological processes or industry norms in this field, which hinders the realization of actual industrial applications.

Facing the above defects, there are many new research directions that provide ideas for solving these problems. In particular, the durability of the superhydrophobic coatings must be improved, otherwise, it is difficult for them to really occupy a place in the field of corrosion protection.

First of all, the use of surface modifiers after the electrodeposition should be avoided. Some modifiers are not only toxic but also easy to fall off. Instead, some low surface energy material which is environmentally friendly can be added to the electrolyte and deposited directly on the surface of the substrate. It is also possible to add more than one kind of particles with hydrophobicity and other special properties to the bath to prepare multi-functional composite coatings, so that the coating can obtain superhydrophobicity, good wear resistance and other properties.

Secondly, the stability of the coating can be improved by optimizing the composition of the plating solution. For example, mussels, as a marine organism, can easily adhere to various substrates by secreting mytilus edulis foot protein-5 (Mefp-5) [223]. Further studies have found that 3,4- levodopa (DOPA) is the main source of such strong adhesion [224]. Wang et al. [112] got inspiration from this phenomenon and added dopamine to the bath. Then multifunctional zinc/polydopamine/n-dodecyl mercaptan (Zn/pDop/NDM) composite superhydrophobic coatings with excellent adhesion were successfully prepared on the surface of Cu, Al and steel. The maximum WCA was 167.6°, and the SA was as low as 1°. At the same time, the excellent adhesion and wear resistance of the coating were proved by cross cut tape test and abrasion test.

The construction of superhydrophobic coating with corrosion inhibitor is also a research direction to improve the durable anti-corrosion performance in the future. The corrosion inhibitor is added to the matrix, and when the superhydrophobicity of the coating is lost, the inhibitor can be released to the surface of the coating to provide long-term corrosion protection. For example, Zhao et al. [225] prepared a SiO_2 superhydrophobic coating co-embedded with corrosion inhibitor benzotriazole (BTA) on the surface of aluminum alloy by electrodeposition. The release of the corrosion inhibitor had a pH response mechanism, which enhanced the durability of the anticorrosive coating.

The preparation of anticorrosive superhydrophobic coatings with self-repairing properties is an important channel to improve durability. In recent years, intelligent coatings with self-repairing properties have

gradually become a research hotspot. If the self-healing property is given to superhydrophobic coatings, the durability of the coatings can be greatly improved. It can be considered from two aspects, to reduce the surface energy of the coating and to restore the damaged surface structure. For instance, Li et al. [226], inspired by the self-healing mechanism of superhydrophobic plants, prepared porous polymer superhydrophobic coatings with self-repairing properties. When the fluorosilane on the surface decomposed or there were scratches on the coating surface, the internal fluorosilane would migrate to the coating surface as a healing agent to restore the hydrophobic function. Qian et al. [227] fabricated a self-healing superhydrophobic coating using shape memory polymers (SMPs). Due to the thermally triggered shape memory effect of the epoxy polymer, the surface morphology of the coating could be restored by heating for 20 min at 60 °C after the surface structure was destroyed, thus repairing the superhydrophobic performance and providing long-term anti-corrosion protection. Previous studies have undoubtedly proved the possibility of preparing self-healing superhydrophobic coatings.

8. Conclusion

The superhydrophobic coatings have excelllent water resistance, thereby effectively isolating corrosive media and achieving excellent anti-corrosion effects. Electrodeposition is an effective method for the preparation of superhydrophobic coatings with the potential for large-scale industrial applications, among which composite electrodeposition has great advantages because it can avoid secondary surface modification and improve the stability of the coating. Crystallization modifiers, current density, and deposition time can greatly affect the hydrophobicity and anti-corrosion performance of coatings fabricated by the electrodeposition process. The new developments including pulse electrodeposition, jet electrodeposition, magnetic field-induced electrodeposition and ultrasound-assisted electrodeposition have great research value. In addition to anti-corrosion, electrodeposition can also be used in the preparation of anti-icing, self-cleaning superhydrophobic coatings, catalysts for water splitting and other fields. Although the prepared coatings still face challenges in terms of stability and durability, by optimizing this technology, superhydrophobic coatings are likely to become a widely used, superior and environmentally friendly anti-corrosion method one day.

Declaration of Competing Interest

The authors declare that they have no known competing financial interests or personal relationships that could have appeared to influence the work reported in this paper.

Acknowledgements

This work was supported by Shandong Provincial Natural Science Foundation, China (No. ZR2019MEM014), the Fundamental Research Funds for the Central Universities (No. 20CX02401A) and the Development Fund of Shandong Key Laboratory of Oil & Gas Storage and Transportation Safety.

References

[1] P. Liu, Y. Gao, F. Wang, J. Yang, X. Yu, W. Zhang, L. Yang, Superhydrophobic and self-cleaning behavior of Portland cement with lotus-leaf-like microstructure, J. Clean. Prod. 156 (2017) 775–785, https://doi.org/10.1016/j.jclepro.2017.03.211.

[2] H. Yoon, H. Kim, S.S. Latthe, M.-w. Kim, S. Al-Deyab, S.S. Yoon, A highly transparent self-cleaning superhydrophobic surface by organosilane-coated alumina particles deposited via electrospraying, J. Mater. Chem. A 3 (2015) 11403–11410, https://doi.org/10.1039/C5TA02226F.

[3] L. Liu, W. Liu, R. Chen, X. Li, X. Xie, Hierarchical growth of Cu zigzag microstrips on Cu foil for superhydrophobicity and corrosion resistance, Chem. Eng. J. 281 (2015) 804–812, https://doi.org/10.1016/j.cej.2015.07.028.

[4] Y. Cheng, T. Zhu, S. Li, J. Huang, J. Mao, H. Yang, S. Gao, Z. Chen, Y. Lai, A novel strategy for fabricating robust superhydrophobic fabrics by environmentally-friendly enzyme etching, Chem. Eng. J. 355 (2019) 290–298, https://doi.org/10.1016/j.cej.2018.08.113.

[5] L. Lv, H. Liu, W. Zhang, J. Chen, Z. Liu, Facile UV-curable fabrication of robust, anti-icing superhydrophobic coatings based on polyurethane, Mater. Lett. 258 (2020) 126653, https://doi.org/10.1016/j.matlet.2019.126653.

[6] M. Liravi, H. Pakzad, A. Moosavi, A. Nouri-Borujerdi, A comprehensive review on recent advances in superhydrophobic surfaces and their applications for drag reduction, Prog. Org. Coat. 140 (2020) 105537, https://doi.org/10.1016/j.porgcoat.2019.105537.

[7] V.S. Saji, Wax-based artificial superhydrophobic surfaces and coatings, Colloids Surf, Physicochem. Eng. Aspects 602 (2020) 125132, , https://doi.org/10.1016/j.colsurfa.2020.125132.

[8] A. Fihri, E. Bovero, A. Al-Shahrani, A. Al-Ghamdi, G. Alabedi, Recent progress in superhydrophobic coatings used for steel protection: a review, Colloids Surf, Physicochem. Eng. Aspects 520 (2017) 378–390, https://doi.org/10.1016/j.colsurfa.2016.12.057.

[9] M. Natesan, N. Palaniswamy, Atmospheric corrosivity and durability maps of India, Corros. Rev. 27 (2009), https://doi.org/10.1515/CORRREV.2009.27.S1.61.

[10] Y. Shao, J. Zhao, Y. Fan, Z. Wan, L. Lu, Z. Zhang, W. Ming, L. Ren, Shape memory superhydrophobic surface with switchable transition between “Lotus effect” to “Rose Petal Effect”, Chem. Eng. J. 382 (2020) 122989, https://doi.org/10.1016/j.cej.2019.122989.

[11] V. Sharma, V. Sharma, M.S. Goyat, A. Hooda, J.K. Pandey, A. Kumar, R. Gupta, A.K. Upadhyay, R. Prakash, J.B. Kirabira, P. Mandal, P.K. Bhargav, Recent progress in nano-oxides and CNTs based corrosion resistant superhydrophobic coatings: a critical review, Prog. Org. Coat. 140 (2020) 105512, https://doi.org/10.1016/j.porgcoat.2019.105512.

[12] J. Li, Z. Jing, Y. Yang, Q. Wang, Z. Lei, From Cassie state to Gecko state: a facile hydrothermal process for the fabrication of superhydrophobic surfaces with controlled sliding angles on zinc substrates, Surf. Coat. Technol. 258 (2014) 973–978, https://doi.org/10.1016/j.surfcoat.2014.07.047.

[13] N. Celik, I. Torun, M. Ruzi, A. Esidir, M. Serdar Onses, Fabrication of robust superhydrophobic surfaces by one-step spray coating: evaporation driven self-assembly of wax and nanoparticles into hierarchical structures, Chem. Eng. J. (2020) 125230, https://doi.org/10.1016/j.cej.2020.125230.

[14] P. Nguyen-Tri, H.N. Tran, C.O. Plamondon, L. Tuduri, D.-V.N. Vo, S. Nanda, A. Mishra, H.-P. Chao, A.K. Bajpai, Recent progress in the preparation, properties and applications of superhydrophobic nano-based coatings and surfaces: a review, Prog. Org. Coat. 132 (2019) 235–256, https://doi.org/10.1016/j.porgcoat.2019.03.042.

[15] M. Khodaei, S. Shadmani, Superhydrophobicity on aluminum through reactive-etching and TEOS/GPTMS/nano-Al_2O_3 silane-based nanocomposite coating, Surf. Coat. Technol. 374 (2019) 1078–1090, https://doi.org/10.1016/j.surfcoat.2019.06.074.

[16] A. Kumar, B. Gogoi, Development of durable self-cleaning superhydrophobic coatings for aluminium surfaces via chemical etching method, Tribol. Int. 122 (2018) 114–118, https://doi.org/10.1016/j.triboint.2018.02.032.

[17] P. Dimitrakellis, E. Gogolides, Atmospheric plasma etching of polymers: a palette of applications in cleaning/ashing, pattern formation, nanotexturing and superhydrophobic surface fabrication, Microelectron. Eng. 194 (2018) 109–115, https://doi.org/10.1016/j.mee.2018.03.017.

[18] W. Somrang, S. Denchitcharoen, P. Eiamchai, M. Horprathum, C. Chananonnawathorn, Superhydrophobic and antireflective surface of nanostructures fabricated by CF_4 plasma etching, Mater. Today: Proc. 5 (2018) 13879–13885, https://doi.org/10.1016/j.matpr.2018.02.033.

[19] W. Liu, Y. Luo, L. Sun, R. Wu, H. Jiang, Y. Liu, Fabrication of the superhydrophobic surface on aluminum alloy by anodizing and polymeric coating, Appl. Surf. Sci. 264 (2013) 872–878, https://doi.org/10.1016/j.apsusc.2012.10.167.

[20] X. Zhou, S. Yu, S. Guan, Z. Lv, E. Liu, Y. Zhao, Fabrication and characterization of superhydrophobic TiO_2 nanotube coating by a facile anodic oxidation approach, Surf. Coat. Technol. 354 (2018) 83–91, https://doi.org/10.1016/j.surfcoat.2018.09.014.

[21] M. Cui, C. Xu, Y. Shen, H. Tian, H. Feng, J. Li, Electrospinning superhydrophobic nanofibrous poly(vinylidene fluoride)/stearic acid coatings with excellent corrosion resistance, Thin Solid Films 657 (2018) 88–94, https://doi.org/10.1016/j.tsf.2018.05.008.

[22] J. Zha, N. Batisse, D. Claves, M. Dubois, A universal fluorous technology toward superhydrophobic coatings, J. Colloid Interface Sci. 553 (2019) 778–787, https://doi.org/10.1016/j.jcis.2019.06.067.

[23] S. Czyzyk, A. Dotan, H. Dodiuk, S. Kenig, Processing effects on the kinetics morphology and properties of hybrid sol-gel superhydrophobic coatings, Prog. Org. Coat. 140 (2020) 105501, https://doi.org/10.1016/j.porgcoat.2019.105501.

[24] R.V. Lakshmi, T. Bharathidasan, B.J. Basu, Superhydrophobic sol–gel nanocomposite coatings with enhanced hardness, Appl. Surf. Sci. 257 (2011) 10421–10426, https://doi.org/10.1016/j.apsusc.2011.06.122.

[25] L. Ni, C. Zhu, S. Zhang, P. Cai, A. Airoudj, L. Vonna, S. Hajjar-Garreau, A. Chemtob, Light-induced crystallization-driven formation of hierarchically ordered superhydrophobic sol-gel coatings, Prog. Org. Coat. 135 (2019) 255–262, https://doi.org/10.1016/j.porgcoat.2019.05.045.

[26] R. Taurino, E. Fabbri, D. Pospiech, A. Synytska, M. Messori, Preparation of scratch resistant superhydrophobic hybrid coatings by sol–gel process, Prog. Org. Coat. 77 (2014) 1635–1641, https://doi.org/10.1016/j.porgcoat.2014.05.009.

[27] J. Xu, Y. Liu, W. Du, W. Lei, X. Si, T. Zhou, J. Lin, L. Peng, Superhydrophobic silica antireflective coatings with high transmittance via one-step sol-gel process, Thin

Solid Films 631 (2017) 193–199, https://doi.org/10.1016/j.tsf.2017.03.005.
[28] H.M. Forooshani, M. Aliofkhazraei, A.S. Rouhaghdam, Superhydrophobic copper surfaces by shot peening and chemical treatment, Surf. Rev. Lett. 24 (2017) 1750093, , https://doi.org/10.1142/S0218625X17500937.
[29] A. Hooda, M.S. Goyat, J.K. Pandey, A. Kumar, R. Gupta, A review on fundamentals, constraints and fabrication techniques of superhydrophobic coatings, Prog. Org. Coat. 142 (2020) 105557, https://doi.org/10.1016/j.porgcoat.2020.105557.
[30] F.C. Walsh, S. Wang, N. Zhou, The electrodeposition of composite coatings: diversity, applications and challenges, Curr Opin Electrochem 20 (2020) 8–19, https://doi.org/10.1016/j.coelec.2020.01.011.
[31] H. Khani, D.O. Wipf, Iron oxide nanosheets and pulse-electrodeposited Ni–Co–S nanoflake arrays for high-performance charge storage, ACS Appl, Mater. Interfaces 9 (2017) 6967–6978, https://doi.org/10.1021/acsami.6b11498.
[32] N. Vourdas, A. Tserepi, A.G. Boudouvis, E. Gogolides, Plasma processing for polymeric microfluidics fabrication and surface modification: effect of super-hydrophobic walls on electroosmotic flow, Microelectron. Eng. 85 (2008) 1124–1127, https://doi.org/10.1016/j.mee.2007.12.032.
[33] R. Akbari, G. Godeau, M. Mohammadizadeh, F. Guittard, T. Darmanin, The influence of bath temperature on the one-step electrodeposition of non- wetting copper oxide coatings, Appl. Surf. Sci. 503 (2020) 144094, https://doi.org/10.1016/j.apsusc.2019.144094.
[34] S.M. Emarati, M. Mozammel, Efficient one-step fabrication of superhydrophobic nano-TiO_2/TMPSi ceramic composite coating with enhanced corrosion resistance on 316L, Ceram. Int. 46 (2020) 1652–1661, https://doi.org/10.1016/j.ceramint.2019.09.137.
[35] Y. Liu, J. Xue, D. Luo, H. Wang, X. Gong, Z. Han, L. Ren, One-step fabrication of biomimetic superhydrophobic surface by electrodeposition on magnesium alloy and its corrosion inhibition, J. Colloid Interface Sci. 491 (2017) 313–320, https://doi.org/10.1016/j.jcis.2016.12.022.
[36] H. Li, S. Yu, X. Han, S. Zhang, Y. Zhao, A simple method for fabrication of bionic superhydrophobic zinc coating with crater-like structures on steel substrate, J. Bionic Eng. 13 (2016) 622–630, https://doi.org/10.1016/S1672-6529(16)60333-5.
[37] M. Salehi, M. Mozammel, S.M. Emarati, Superhydrophobic and corrosion resistant properties of electrodeposited Ni-TiO_2/TMPSi nanocomposite coating, Colloids Surf. Physicochem. Eng. Aspects 573 (2019) 196–204, https://doi.org/10.1016/j.colsurfa.2019.04.024.
[38] J. Tam, Z. Jiao, J.C.F. Lau, U. Erb, Wear stability of superhydrophobic nano Ni-PTFE electrodeposits, Wear 374-375 (2017) 1–4, https://doi.org/10.1016/j.wear.2016.12.023.
[39] S. Jiang, Z. Guo, Y. Deng, H. Dong, X. Li, J. Liu, Effect of pulse frequency on the one-step preparation of superhydrophobic surface by pulse electrodeposition, Appl. Surf. Sci. 458 (2018) 603–611, https://doi.org/10.1016/j.apsusc.2018.07.120.
[40] S. Jiang, Z. Guo, G.K. Gyimah, C. Zhang, G. Liu, Preparation of biomimetic superhydrophobic surface by a facile one-step pulse electrodeposition, Procedia Cirp 68 (2018) 237–241, https://doi.org/10.1016/j.procir.2017.12.055.
[41] Y. Zhang, T. Lin, Influence of duty cycle on properties of the superhydrophobic coating on an anodized magnesium alloy fabricated by pulse electrodeposition, Colloids Surf, Physicochem. Eng. Aspects 568 (2019) 43–50, https://doi.org/10.1016/j.colsurfa.2019.01.078.
[42] W. Cui, K. Wang, F. Xia, P. Wang, Simulation and characterization of Ni–doped SiC nanocoatings prepared by jet electrodeposition, Ceram. Int. 44 (2018) 5500–5505, https://doi.org/10.1016/j.ceramint.2017.12.189.
[43] W. Jiang, L. Shen, M. Qiu, X. Wang, M. Fan, Z. Tian, Preparation of Ni-SiC composite coatings by magnetic field-enhanced jet electrodeposition, J. Alloys. Compd. 762 (2018) 115–124, https://doi.org/10.1016/j.jallcom.2018.05.097.
[44] W. Jiang, L. Shen, M. Xu, Z. Wang, Z. Tian, Mechanical properties and corrosion resistance of Ni-Co-SiC composite coatings by magnetic field-induced jet electrodeposition, J. Alloys. Compd. 791 (2019) 847–855, https://doi.org/10.1016/j.jallcom.2019.03.391.
[45] X. Liu, L. Shen, M. Qiu, Z. Tian, Y. Wang, K. Zhao, Jet electrodeposition of nanocrystalline nickel assisted by controllable friction, Surf. Coat. Technol. 305 (2016) 231–240, https://doi.org/10.1016/j.surfcoat.2016.08.043.
[46] D. Ning, A. Zhang, M. Murtaza, H. Wu, Effect of surfactants on the electrodeposition of Cu-TiO_2 composite coatings prepared by jet electrodeposition, J. Alloys. Compd. 777 (2019) 1245–1250, https://doi.org/10.1016/j.jallcom.2018.11.077.
[47] G. Qiao, T. Jing, N. Wang, Y. Gao, X. Zhao, J. Zhou, W. Wang, High-speed jet electrodeposition and microstructure of nanocrystalline Ni–Co alloys, Electrochim. Acta 51 (2005) 85–92, https://doi.org/10.1016/j.electacta.2005.03.050.
[48] C. Wang, L. Shen, M. Qiu, Z. Tian, W. Jiang, Characterizations of Ni-CeO_2 nanocomposite coating by interlaced jet electrodeposition, J. Alloys. Compd. 727 (2017) 269–277, https://doi.org/10.1016/j.jallcom.2017.08.105.
[49] F.F. Xia, W.C. Jia, C.Y. Ma, R. Yang, Y. Wang, M. Potts, Synthesis and characterization of Ni-doped TiN thin films deposited by jet electrodeposition, Appl. Surf. Sci. 434 (2018) 228–233, https://doi.org/10.1016/j.apsusc.2017.10.203.
[50] B. Li, T. Mei, D. Li, S. Du, Ultrasonic-assisted electrodeposition of Ni-Cu/TiN composite coating from sulphate-citrate bath: structural and electrochemical properties, Ultrason. Sonochem. 58 (2019) 104680, https://doi.org/10.1016/j.ultsonch.2019.104680.
[51] B. Li, W. Zhang, Facile synthesis and electrochemical properties of a novel Ni-B/TiC composite coating via ultrasonic-assisted electrodeposition, Ultrason. Sonochem. 61 (2020) 104837, https://doi.org/10.1016/j.ultsonch.2019.104837.
[52] T.T. Li, L. Ling, M.C. Lin, Q. Jiang, Q. Lin, C.W. Lou, J.H. Lin, Effects of ultrasonic treatment and current density on the properties of hydroxyapatite coating via electrodeposition and its in vitro biomineralization behavior, Mater. Sci. Eng. C 105 (2019) 110062, https://doi.org/10.1016/j.msec.2019.110062.
[53] L. Ling, T.T. Li, M.C. Lin, Q. Jiang, H.T. Ren, C.W. Lou, J.H. Lin, Effect of hydrogen peroxide concentration on the nanostructure of hydroxyapatite coatings via ultrasonic-assisted electrodeposition, Mater. Lett. 261 (2020) 126989, , https://doi.org/10.1016/j.matlet.2019.126989.
[54] F.F. Xia, C.H. Ma, Y.F. Yin, L. Miao, A study on Ni–TiN coatings produced by ultrasonic pluse electrodeposition, Adv. Mat. Res. 562-564 (2012) 269–272, https://doi.org/10.4028/www.scientific.net/AMR.562-564.269.
[55] H. Zhang, N. Zhang, F. Fang, Fabrication of high-performance nickel/graphene oxide composite coatings using ultrasonic-assisted electrodeposition, Ultrason. Sonochem. 62 (2020) 104858, https://doi.org/10.1016/j.ultsonch.2019.104858.
[56] M. Huang, G. Marinaro, X. Yang, B. Fritzsche, Z. Lei, M. Uhlemann, K. Eckert, G. Mutschke, Mass transfer and electrolyte flow during electrodeposition on a conically shaped electrode under the influence of a magnetic field, J. Electroanal. Chem. Lausanne (Lausanne) 842 (2019) 203–213, https://doi.org/10.1016/j.jelechem.2019.04.043.
[57] A. Krause, J. Koza, A. Ispas, M. Uhlemann, A. Gebert, A. Bund, Magnetic field induced micro-convective phenomena inside the diffusion layer during the electrodeposition of Co, Ni and Cu, Electrochim. Acta 52 (2007) 6338–6345, https://doi.org/10.1016/j.electacta.2007.04.054.
[58] H. Matsushima, H. Takahashi, T. Suzuki, M. Ueda, I. Mogi, Effect of a high magnetic field on aluminum electrodeposition using an ionic liquid, Electrochem. commun. 115 (2020) 106733, https://doi.org/10.1016/j.elecom.2020.106733.
[59] L. Shen, M. Xu, W. Jiang, M. Qiu, M. Fan, G. Ji, Z. Tian, A novel superhydrophobic Ni/Nip coating fabricated by magnetic field induced selective scanning electrodeposition, Appl. Surf. Sci. 489 (2019) 25–33, https://doi.org/10.1016/j.apsusc.2019.05.335.
[60] D. Yin, H.A. Murdoch, B. Chad Hornbuckle, E. Hernández-Rivera, M.K. Dunstan, Investigation of anomalous copper hydride phase during magnetic field-assisted electrodeposition of copper, Electrochem. commun. 98 (2019) 96–100, https://doi.org/10.1016/j.elecom.2018.11.018.
[61] T. Darmanin, F. Guittard, Wettability of conducting polymers: from superhydrophilicity to superoleophobicity, Prog. Polym. Sci. 39 (2014) 656–682, https://doi.org/10.1016/j.progpolymsci.2013.10.003.
[62] T.A. Otitoju, A.L. Ahmad, B.S. Ooi, Superhydrophilic (superwetting) surfaces: a review on fabrication and application, J. Ind. Eng. Chem. 47 (2017) 19–40, https://doi.org/10.1016/j.jiec.2016.12.016.
[63] N.J. Shirtcliffe, G. McHale, S. Atherton, M.I. Newton, An introduction to superhydrophobicity, Adv. Colloid Interface Sci. 161 (2010) 124–138, https://doi.org/10.1016/j.cis.2009.11.001.
[64] E. Celia, T. Darmanin, E. Taffin de Givenchy, S. Amigoni, F. Guittard, Recent advances in designing superhydrophobic surfaces, J. Colloid Interface Sci. 402 (2013) 1–18, https://doi.org/10.1016/j.jcis.2013.03.041.
[65] X. Gao, Z. Guo, Biomimetic superhydrophobic surfaces with transition metals and their oxides: a review, J. Bionic Eng. 14 (2017) 401–439, https://doi.org/10.1016/S1672-6529(16)60408-0.
[66] M. Yeganeh, N. Mohammadi, Superhydrophobic surface of Mg alloys: a review, J. Magnes. Alloy. 6 (2018) 59–70, https://doi.org/10.1016/j.jma.2018.02.001.
[67] E. Orowan, Surface energy and surface tension in solids and liquids, Proc. R. Soc. Lond. 316 (1970) 473–491, https://doi.org/10.1098/rspa.1970.009.
[68] H.Y. Erbil, S. Katrina, B.L. Ruth, Surface chemistry of solid and liquid interfaces, Blackwell Pub.2006. https://doi.org/10.1002/9781444305401.ch9.
[69] S.W. Ip, J.M. Toguri, The equivalency of surface tension, surface energy and surface free energy, J. Mater. Sci. 29 (1994) 688–692, https://doi.org/10.1007/BF00445980.
[70] E.J. Chibowski, Surface free energy and wettability of silyl layers on silicon determined from contact angle hysteresis, Adv. Colloid Interface Sci. 113 (2005) 121–131, https://doi.org/10.1016/j.cis.2005.01.005.
[71] C.X. Wang, X.F. Zhang, A non-particle and fluorine-free superhydrophobic surface based on one-step electrodeposition of dodecyltrimethoxysilane on mild steel for corrosion protection, Corros. Sci. 163 (2020) 108284, https://doi.org/10.1016/j.corsci.2019.108284.
[72] K. Uneyama, Functionalized fluoroalkyl and alkenyl silanes: preparations, reactions, and synthetic applications, J. Fluorine Chem. 129 (2008) 550–576, https://doi.org/10.1016/j.jfluchem.2008.05.012.
[73] G. Barati Darband, M. Aliofkhazraei, S. Khorsand, S. Sokhanvar, A. Kaboli, Science and engineering of superhydrophobic surfaces: review of corrosion resistance, chemical and mechanical stability, Arab. J. Chem. 13 (2020) 1763–1802, https://doi.org/10.1016/j.arabjc.2018.01.013.
[74] E. Rahimi, A. Rafsanjani-Abbasi, A. Kiani-Rashid, H. Jafari, A. Davoodi, Morphology modification of electrodeposited superhydrophobic nickel coating for enhanced corrosion performance studied by AFM, SEM-EDS and electrochemical measurements, Colloids Surf, Physicochem. Eng. Aspects 547 (2018) 81–94, https://doi.org/10.1016/j.colsurfa.2018.03.045.
[75] L. Shen, M. Fan, M. Qiu, W. Jiang, Z. Wang, Superhydrophobic nickel coating fabricated by scanning electrodeposition, Appl. Surf. Sci. 483 (2019) 706–712, https://doi.org/10.1016/j.apsusc.2019.04.019.
[76] Z. Wang, L. Shen, W. Jiang, M. Fan, D. Liu, J. Zhao, Superhydrophobic nickel coatings fabricated by scanning electrodeposition on stainless steel formed by selective laser melting, Surf. Coat. Technol. 377 (2019) 124886, https://doi.org/10.1016/j.surfcoat.2019.08.015.
[77] F.C. Cebeci, Z. Wu, L. Zhai, R.E. Cohen, M.F. Rubner, Nanoporosity-driven superhydrophilicity: a means to create multifunctional antifogging coatings, Langmuir 22 (2006) 2856–2862, https://doi.org/10.1021/la053182p.

[78] M. Qu, G. Zhao, X. Cao, J. Zhang, Biomimetic fabrication of lotus-leaf-like structured polyaniline film with stable superhydrophobic and sonductive properties, Langmuir 24 (2008) 4185–4189, https://doi.org/10.1021/la703284f.

[79] T. Young, An essay on the cohesion of fluids, Philos. Trans. R. Soc. London 1 (1832) 65–87, https://doi.org/10.1098/rspl.1800.0095.

[80] R.N. Wenzel, Resistance of solid surfaces to wetting by water, Trans. Faraday Soc. 28 (1936) 988–994, https://doi.org/10.1021/ie50320a024.

[81] A. Cassie, S. Baxter, Wettability of porous surfaces, Trans. Faraday Soc. 40 (1944) 546–551, https://doi.org/10.1039/TF9444000546.

[82] M. Ji, Researching Advances in application of bio-inspired superhydrophobic metallic surface, Equipment Environmental Engineering 14 (2017) 98–104, https://doi.org/10.7643/issn.1672-9242.2017.10.019.

[83] A. Marmur, Wetting on hydrophobic rough surfaces: To be heterogeneous or not to be? Langmuir 19 (2003) 8343–8348, https://doi.org/10.1021/la0344682.

[84] A. Marmur, Soft contact: measurement and interpretation of contact angles, Soft Matter 2 (2006) 12–17, https://doi.org/10.1039/B514811C.

[85] J. Bico, U. Thiele, D. Quéré, Wetting of textured surfaces, Colloids Surf. Physicochem. Eng. Aspects 206 (2002) 41–46, https://doi.org/10.1016/S0927-7757(02)00061-4.

[86] S. Wang, L. Jiang, Definition of superhydrophobic states, Adv. Mater. 19 (2007) 3423–3424, https://doi.org/10.1002/adma.200700934.

[87] T.G. Cha, J. Yi, M.W. Moon, K.R. Lee, H.Y. Kim, Nanoscale patterning of microtextured surfaces to control superhydrophobic robustness, Langmuir 26 (2010) 8319–8326, https://doi.org/10.1021/la9047402.

[88] H. Wu, K. Zhu, B. Wu, J. Lou, Z. Zhang, G. Chai, Influence of structured sidewalls on the wetting states and superhydrophobic stability of surfaces with dual-scale roughness, Appl. Surf. Sci. 382 (2016) 111–120, https://doi.org/10.1016/j.apsusc.2016.04.101.

[89] B.B. Wu, H.P. Wu, Z. Zhang, C.C. Dong, G.Z. Chai, Thermodynamic analysis of stable wetting states and wetting transition of micro/nanoscale structured surface, Wuli Xuebao/Acta Physica Sinica 64 (2015), https://doi.org/10.7498/aps.64.176801.

[90] B. Bhushan, M. Nosonovsky, The rose petal effect and the modes of superhydrophobicity, Philos. Trans. Math. Phys. Eng. Sci. 368 (2010) 4713–4728, https://doi.org/10.1098/rsta.2010.0203.

[91] E. Bormashenko, Progress in understanding wetting transitions on rough surfaces, Adv. Colloid Interface Sci. 222 (2015) 92–103, https://doi.org/10.1016/j.cis.2014.02.009.

[92] A. Amirfazli, A.W. Neumann, Status of the three-phase line tension: a review, Adv. Colloid Interface Sci. 110 (2004) 121–141, https://doi.org/10.1016/j.cis.2004.05.001.

[93] E. Bormashenko, Boruvka–Neumann Young, Wenzel and Cassie–Baxter equations as the transversality conditions for the variational problem of wetting, Colloids Surf. Physicochem. Eng. Aspects 345 (2009) 163–165, https://doi.org/10.1016/j.colsurfa.2009.04.054.

[94] A. Checco, P. Guenoun, J. Daillant, Nonlinear dependence of the contact angle of nanodroplets on contact line curvature, Phys. Rev. Lett. 91 (2003) 186101, , https://doi.org/10.1103/PhysRevLett.91.186101.

[95] T. Pompe, A. Fery, S. Herminghaus, Measurement of contact line tension by analysis of the three phase boundary with nanometer resolution, J. Adhes. Sci. Technol. 13 (1999) 1155–1164, https://doi.org/10.1163/156856199X00848.

[96] A. Marmur, Line tension and the intrinsic contact angle in solid–liquid–fluid systems, J. Colloid Interface Sci. 186 (1997) 462–466, https://doi.org/10.1006/jcis.1996.4666.

[97] K.D. Humfeld, S. Garoff, Geometry-driven wetting transition, Langmuir 20 (2004) 9223–9226, https://doi.org/10.1021/la048614v.

[98] F. Liu, Y. Deng, X. Han, W. Hu, C. Zhong, Electrodeposition of metals and alloys from ionic liquids, J. Alloys. Compd. 654 (2016) 163–170, https://doi.org/10.1016/j.jallcom.2015.09.137.

[99] A. Bouyelfane, A. Zerga, Ni/Cu electroplating, a worthwhile alternative to use instead of Ag screen-printed front side metallization of conventional solar cells, Mater. Sci. Semicond. Process. 26 (2014) 312–319, https://doi.org/10.1016/j.mssp.2014.05.012.

[100] F. Li, Z. Liu, T. Sun, C. Yang, W. Sun, X. Sun, Y. Ma, X. Ding, In situ analysis of electrocrystallization process of metal electrodeposition with confocal energy dispersive X-ray diffraction based on polycapillary X-ray optics, Nucl. Instrum. Meth. A .785 (2015) 201–205, https://doi.org/10.1016/j.nima.2015.03.015.

[101] P. Allongue, F. Maroun, Metal electrodeposition on single crystal metal surfaces mechanisms, structure and applications, Curr. Opin. Solid State Mater. Sci. 10 (2006) 173–181, https://doi.org/10.1016/j.cossms.2007.04.001.

[102] F. Hao, A. Verma, P.P. Mukherjee, Electrodeposition stability of metal electrodes, Energy Stor. Mater. 20 (2019) 1–6, https://doi.org/10.1016/j.ensm.2019.05.004.

[103] Y. Huang, X. Wu, L. Nie, S. Chen, Z. Sun, Y. He, W. Liu, Mechanism of lithium electrodeposition in a magnetic field, Solid State Ion. 345 (2020) 115171, , https://doi.org/10.1016/j.ssi.2019.115171.

[104] M. Ilieva, V. Tsakova, Copper electrocrystallization in PEDOT in presence and absence of copper–polymer-stabilized species, Electrochim. Acta 50 (2005) 1669–1674, https://doi.org/10.1016/j.electacta.2004.10.018.

[105] Z. Grubač, M. Metikoš-Huković, R. Babić, Electrocrystallization, growth and characterization of calcium phosphate ceramics on magnesium alloys, Electrochim. Acta 109 (2013) 694–700, https://doi.org/10.1016/j.electacta.2013.07.095.

[106] J. Kelber, S. Rudenja, C. Bjelkevig, Electrodeposition of copper on Ru(0001) in sulfuric acid solution: growth kinetics and nucleation behavior, Electrochim. Acta 51 (2006) 3086–3090, https://doi.org/10.1016/j.electacta.2005.08.043.

[107] B. Scharifker, G. Hills, Theoretical and experimental studies of multiple nucleation, Electrochim. Acta 28 (1983) 879–889, https://doi.org/10.1016/0013-4686(83)85163-9.

[108] A. Milchev, I. Krastev, Two-dimensional progressive and instantaneous nucleation with overlap: the case of multi-step electrochemical reactions, Electrochim. Acta 56 (2011) 2399–2403, https://doi.org/10.1016/j.electacta.2010.11.025.

[109] N. Sotskaya, L. Sapronova, O. Dolgikh, Kinetics of the nucleation and growth of nickel particles in α-alanine-containing electrolytes, Prot. Met. Phys. Chem. Surf. 50 (2014), https://doi.org/10.1134/S2070205114010134.

[110] N. Sotskaya, L. Sapronova, O. Dolgikh, Kinetics of nickel electrocrystallization from serine-containing electrolytes, Russ. J. Electrochem. 50 (2014) 1137–1141 https://doi.org/1141.10.1134/S1023193514120106.

[111] N.P. Wasekar, A.P. O'Mullane, G. Sundararajan, A new model for predicting the grain size of electrodeposited nanocrystalline nickel coatings containing sulphur, phosphorus or boron based on typical systems, J. Electroanal. Chem. 833 (2019) 198–204, https://doi.org/10.1016/j.jelechem.2018.11.057.

[112] H. Wang, Y. Zhu, Z. Hu, X. Zhang, S. Wu, R. Wang, Y. Zhu, A novel electrodeposition route for fabrication of the superhydrophobic surface with unique self-cleaning, mechanical abrasion and corrosion resistance properties, Chem. Eng. J. 303 (2016) 37–47, https://doi.org/10.1016/j.cej.2016.05.133.

[113] A.C.C. de Leon, R.B. Pernites, R.C. Advincula, Superhydrophobic colloidally textured polythiophene film as superior anticorrosion coating, ACS Appl. Mater. Interfaces 4 (2012) 3169–3176, https://doi.org/10.1021/am300513e.

[114] E. Liu, X. Yin, J. Hu, S. Yu, Y. Zhao, W. Xiong, Fabrication of a biomimetic hierarchical superhydrophobic Cu-Ni coating with self-cleaning and anti-corrosion properties, Colloids Surf, Physicochem. Eng. Aspects 586 (2020) 124223, , https://doi.org/10.1016/j.colsurfa.2019.124223.

[115] R. Farahati, H. Behzadi, S.M. Mousavi-Khoshdel, A. Ghaffarinejad, Evaluation of corrosion inhibition of 4-(pyridin-3-yl) thiazol-2-amine for copper in HCl by experimental and theoretical studies, J. Mol. Struct. 1205 (2020) 127658, , https://doi.org/10.1016/j.molstruc.2019.127658.

[116] T. Ma, B. Tan, Y. Xu, D. Yin, G. Liu, N. Zeng, G. Song, Z. Kao, Y. Liu, Corrosion control of copper wiring by barrier CMP slurry containing azole inhibitor: combination of simulation and experiment, Colloids Surf. Physicochem. Eng. Aspects 599 (2020) 124872, , https://doi.org/10.1016/j.colsurfa.2020.124872.

[117] X. Yu, Z. Wang, Z. Lu, Atmospheric corrosion behavior of copper under static magnetic field environment, Mater. Lett. 266 (2020) 127472, https://doi.org/10.1016/j.matlet.2020.127472.

[118] P. Yi, C. Dong, K. Xiao, X. Li, Surface failure analysis of a field-exposed copper-clad plate in a marine environment with industrial pollution, Appl. Surf. Sci. 399 (2017) 608–616, https://doi.org/10.1016/j.apsusc.2016.12.118.

[119] S. Khorsand, K. Raeissi, F. Ashrafizadeh, Corrosion resistance and long-term durability of super-hydrophobic nickel film prepared by electrodeposition process, Appl. Surf. Sci. 305 (2014) 498–505, https://doi.org/10.1016/j.apsusc.2014.03.123.

[120] T.B. Abbott, Magnesium: Industrial and research developments over the last 15 years, Corrosion 71 (2014) 120–127, https://doi.org/10.5006/1474.

[121] Rc. Zeng, J. Zhang, Wj. Huang, W. Dietzel, K.U. Kainer, C. Blawert, W. Ke, Review of studies on corrosion of magnesium alloys, Trans. Nonferrous Met. Soc. China 16 (2006) s763–s771, https://doi.org/10.1016/S1003-6326(06)60297-5.

[122] Z. She, X. Mou, L. Wang, J. He, Research progress of the superhydrophobic surfaces for improving the corrosion resistance of magnesium alloy, Equipment Environmental Engineering 13 (2016) 120–129, https://doi.org/10.7643/issn.1672-9242.2016.06.021.

[123] X. Liu, T.C. Zhang, H. He, L. Ouyang, S. Yuan, A stearic Acid/CeO_2 bilayer coating on AZ31B magnesium alloy with superhydrophobic and self-cleaning properties for corrosion inhibition, J. Alloys. Compd. 834 (2020) 155210, , https://doi.org/10.1016/j.jallcom.2020.155210.

[124] T. Zheng, Y. Hu, F. Pan, Y. Zhang, A. Tang, Fabrication of corrosion-resistant superhydrophobic coating on magnesium alloy by one-step electrodeposition method, J. Magnes. Alloy. 7 (2019) 193–202, https://doi.org/10.1016/j.jma.2019.05.006.

[125] N. Xu, D.K. Sarkar, X.G. Chen, W.P. Tong, Corrosion performance of superhydrophobic nickel stearate/nickel hydroxide thin films on aluminum alloy by a simple one-step electrodeposition process, Surf. Coat. Technol. 302 (2016) 173–184, https://doi.org/10.1016/j.surfcoat.2016.05.050.

[126] D. Zhang, L. Li, Y. Wu, B. Zhu, H. Song, One-step method for fabrication of bioinspired hierarchical superhydrophobic surface with robust stability, Appl. Surf. Sci. 473 (2019) 493–499, https://doi.org/10.1016/j.apsusc.2018.12.174.

[127] J. Liang, D. Li, D. Wang, K. Liu, L. Chen, Preparation of stable superhydrophobic film on stainless steel substrate by a combined approach using electrodeposition and fluorinated modification, Appl. Surf. Sci. 293 (2014) 265–270, https://doi.org/10.1016/j.apsusc.2013.12.147.

[128] M. Xiang, M. Jiang, Y. Zhang, Y. Liu, F. Shen, G. Yang, Y. He, L. Wang, X. Zhang, S. Deng, Fabrication of a novel superhydrophobic and superoleophilic surface by one-step electrodeposition method for continuous oil/water separation, Appl. Surf. Sci. 434 (2018) 1015–1020, https://doi.org/10.1016/j.apsusc.2017.10.183.

[129] T. Xiang, D. Chen, Z. Lv, Z. Yang, L. Yang, C. Li, Robust superhydrophobic coating with superior corrosion resistance, J. Alloys. Compd. 798 (2019) 320–325, https://doi.org/10.1016/j.jallcom.2019.05.187.

[130] H. Li, S. Yu, J. Hu, X. Yin, Modifier-free fabrication of durable superhydrophobic electrodeposited Cu-Zn coating on steel substrate with self-cleaning, anti-corrosion and anti-scaling properties, Appl. Surf. Sci. 481 (2019) 872–882, https://doi.org/10.1016/j.apsusc.2019.03.123.

[131] Y. Fan, Y. He, P. Luo, X. Chen, B. Liu, A facile electrodeposition process to fabricate corrosion-resistant superhydrophobic surface on carbon steel, Appl. Surf. Sci. 368 (2016) 435–442, https://doi.org/10.1016/j.apsusc.2016.01.252.

[132] Z. Yu, C. Zhou, R. Liu, Q. Zhang, J. Gong, D. Tao, Z. Ji, Fabrication of superhydrophobic surface with enhanced corrosion resistance on H62 brass substrate, Colloids Surf, Physicochem. Eng. Aspects 589 (2020) 124475, , https://doi.org/10.1016/j.colsurfa.2020.124475.
[133] Z. Kang, W. Li, Facile and fast fabrication of superhydrophobic surface on magnesium alloy by one-step electrodeposition method, J Ind Eng Chem 50 (2017) 50–56, https://doi.org/10.1016/j.jiec.2017.01.016.
[134] H. Wang, S. Dong, Z. Wang, One-step fabrication of superhydrophobic surface on beryllium copper alloys and corrosion protection application, Colloids Surf, Physicochem. Eng. Aspects 556 (2018) 291–298, https://doi.org/10.1016/j.colsurfa.2018.08.044.
[135] W. Xu, K. Rajan, X.G. Chen, D.K. Sarkar, Facile electrodeposition of superhydrophobic aluminum stearate thin films on copper substrates for active corrosion protection, Surf. Coat. Technol. 364 (2019) 406–415, https://doi.org/10.1016/j.surfcoat.2019.02.070.
[136] G. He, S. Lu, W. Xu, P. Ye, G. Liu, H. Wang, T. Dai, Stable superhydrophobic Zn/ZnO surfaces fabricated via electrodeposition on tin substrate for self-cleaning behavior and switchable wettability, J. Alloys. Compd. 747 (2018) 772–782, https://doi.org/10.1016/j.jallcom.2018.03.108.
[137] L. Xu, D. Wei, Y. Chen, R. Li, A feasible electrochemical method for tuning coatings wettability from superhydrophilicity to superhydrophobicity, Appl. Surf. Sci. 385 (2016) 80–87, https://doi.org/10.1016/j.apsusc.2016.05.053.
[138] T. Darmanin, F. Guittard, Superhydrophobic fiber mats by electrodeposition of fluorinated Poly(3,4-ethyleneoxythiathiophene), J. Am. Chem. Soc. 133 (2011) 15627–15634, https://doi.org/10.1021/ja205283b.
[139] T. Darmanin, F. Guittard, Superhydrophobic surface properties with various nanofibrous structures by electrodeposition of PEDOT polymers with short fluorinated chains and rigid spacers, Synth. Met. 205 (2015) 58–63, https://doi.org/10.1016/j.synthmet.2015.03.029.
[140] C.J. Weng, C.H. Chang, C.W. Peng, S.W. Chen, J.M. Yeh, C.L. Hsu, Y. Wei, K.C. Chang, Advanced anticorrosive coatings prepared from the mimicked xanthosoma sagittifolium-leaf-like electroactive epoxy with synergistic effects of superhydrophobicity and redox catalytic capability, Chem. Mater. 23 (2011) 2075–2083, https://doi.org/10.1021/cm1030377.
[141] N. Guo, Y. Yin, J. Ren, C. Wang, Superhydrophobic mechanism and property of fluoride-free hydrosol in-situ deposition driven by electrochemistry on cotton fabrics, J. Text. Des. Res. 36 (2015) 92–97, https://doi.org/10.13475/j. fzxb.20140806206.
[142] E.L. Foster, A.C.C. De Leon, J. Mangadlao, R. Advincula, Electropolymerized and polymer grafted superhydrophobic, superoleophilic, and hemi-wicking coatings, J. Mater. Chem. 22 (2012) 11025–11031, https://doi.org/10.1039/C2JM31067H.
[143] M. Nicolas, Acids and alkali resistant sticky superhydrophobic surfaces by one-pot electropolymerization of perfluoroalkyl alkyl pyrrole, J. Colloid Interface Sci. 343 (2010) 608–614, https://doi.org/10.1016/j.jcis.2009.11.052.
[144] T. Darmanin, F. Guittard, pH- and voltage-switchable superhydrophobic surfaces by electro-copolymerization of EDOT derivatives containing carboxylic acids and long alkyl chains, Chemphyschem. 14 (2013) 2529–2533, https://doi.org/10.1002/cphc.201300283.
[145] G. Ramos Chagas, G. Morán Cruz, R. Méallet-Renault, A. Gaucher, D. Prim, D.E. Weibel, S. Amigoni, F. Guittard, T. Darmanin, Superhydrophobic and fluorescent properties of fluorinated polypyrene surfaces using various polar linkers prepared via electropolymerization, React. Funct. Polym. 135 (2019) 65–76, https://doi.org/10.1016/j.reactfunctpolym.2018.12.001.
[146] F.C. Walsh, Modern developments in electrodes for electrochemical technology and the role of surface finishing, Trans. Inst. Met. Finish. 97 (2019) 28–42, https://doi.org/10.1080/00202967.2019.1551277.
[147] K. Helle, F. Walsh, Electrodeposition of composite layers consisting of inert inclusions in a metal matrix, Trans. Inst. Metal Finish 75 (1997) 53–58, https://doi.org/10.1080/00202967.1997.11871143.
[148] N. Guglielmi, Kinetics of the deposition of inert particles from electrolytic baths, J. Electrochem. Soc. 119 (1972) 1009–1012, https://doi.org/10.1149/1.2404383.
[149] C.T.J. Low, R.G.A. Wills, F.C. Walsh, Electrodeposition of composite coatings containing nanoparticles in a metal deposit, Surf. Coat. Technol. 201 (2006) 371–383, https://doi.org/10.1016/j.surfcoat.2005.11.123.
[150] B. Losiewicz, Electrodeposition mechanism of composite coatings, Solid State Phenom. 228 (2015) 65–78, https://doi.org/10.4028/www.scientific.net/SSP.228.65.
[151] J.P. Celis, J. Roos, C. Buelens, A mathematical model for the electrolytic codeposition of particles in a metallic matrix, J. Electrochem. Soc. 134 (1987) 1402–1408, https://doi.org/10.1149/1.2100680.
[152] J.Bing Hwang, Mechanism of codeposition of silicon carbide with electrolytic cobalt, J. Electrochem. Soc. 140 (1993) 979, https://doi.org/10.1149/1.2056239.
[153] J. Fransaer, J.-P. Celis, J. Roos, Analysis of the electrolytic codeposition of non-brownian particles with metals, J. Electrochem. Soc. 139 (1992) 413–425, https://doi.org/10.1149/1.2069233.
[154] S.K. Tiwari, V. Kumar, A. Huczko, R. Oraon, A.D. Adhikari, G.C. Nayak, Magical allotropes of carbon: prospects and applications, Crit. Rev. Solid State Mater. Sci. 41 (2016) 257–317, https://doi.org/10.1080/10408436.2015.1127206.
[155] C. Feng, Z. Yi, F. She, W. Gao, Z. Peng, C.J. Garvey, L.F. Dumée, L. Kong, Superhydrophobic and superoleophilic micro-wrinkled reduced graphene oxide as a highly portable and recyclable oil sorbent, ACS Appl. Mater. Interfaces 8 (2016) 9977–9985, https://doi.org/10.1021/acsami.6b01648.
[156] B. Choi, H.S. Park, Superhydrophobic graphene/nafion nanohybrid films with hierarchical roughness, J. Phys. Chem. C 116 (2012), https://doi.org/10.1021/jp207818b.
[157] S. Ding, T. Xiang, C. Li, S. Zheng, J. Wang, M. Zhang, C. Dong, W. Chan, Fabrication of self-cleaning super-hydrophobic nickel/graphene hybrid film with improved corrosion resistance on mild steel, Mater. Des. 117 (2017) 280–288, https://doi.org/10.1016/j.matdes.2016.12.084.
[158] Z. Bai, B. Zhang, Fabrication of superhydrophobic reduced-graphene oxide/nickel coating with mechanical durability, self-cleaning and anticorrosion performance, Nano Materials Science. 2 (2019) 151–158, https://doi.org/10.1016/j.nanoms.2019.05.001.
[159] Ms. Goyat, V. Jaglan, V. Tomar, G. Louchaert, A. Kumar, K. Kumar, A. Singla, R. Gupta, D. Bhan, S. Rai, S. Sharma, Superior thermomechanical and wetting properties of ultrasonic dual mode mixing assisted epoxy-CNT nanocomposites, High Perform, Polym. (2017) 095400831774902, , https://doi.org/10.1177/0954008317749021.
[160] M.F.L. De Volder, S.H. Tawfick, R.H. Baughman, A.J. Hart, Carbon nanotubes: present and future commercial applications, Science 339 (2013) 535–539, https://doi.org/10.1126/science.1222453.
[161] S. Barthwal, S. Barthwal, B. Singh, N. Bahadur Singh, Multifunctional and fluorine-free superhydrophobic composite coating based on PDMS modified MWCNTs/ZnO with self-cleaning, oil-water separation, and flame retardant properties, Colloids Surf, Physicochem. Eng. Aspects 597 (2020) 124776, https://doi.org/10.1016/j.colsurfa.2020.124776.
[162] S. Zhou, X. Zhu, L. Ma, Q. Yan, S. Wang, Outstanding superhydrophobicity and corrosion resistance on carbon-based film surfaces coupled with multi-walled carbon nanotubes and nickel nano-particles, Surf. Sci. 677 (2018) 193–202, https://doi.org/10.1016/j.susc.2018.07.010.
[163] X. Zhu, S. Zhou, Q. Yan, S. Wang, Multi-walled carbon nanotubes enhanced superhydrophobic MWCNTs-Co/a-C:H carbon-based film for excellent self-cleaning and corrosion resistance, Diamond Relat. Mater. 86 (2018) 87–97, https://doi.org/10.1016/j.diamond.2018.04.021.
[164] S. Feng, Z. Zhong, Y. Wang, W. Xing, E. Drioli, Progress and perspectives in PTFE membrane: preparation, modification, and applications, J. Membr. Sci. 549 (2018) 332–349, https://doi.org/10.1016/j.memsci.2017.12.032.
[165] D. Iacovetta, J. Tam, U. Erb, Synthesis, structure, and properties of superhydrophobic nickel–PTFE nanocomposite coatings made by electrodeposition, Surf. Coat. Technol. 279 (2015) 134–141, https://doi.org/10.1016/j.surfcoat.2015.08.022.
[166] J. Zhou, G. Zhao, J. Li, J. Chen, S. Zhang, J. Wang, F.C. Walsh, S. Wang, Y. Xue, Electroplating of non-fluorinated superhydrophobic Ni/WC/WS_2 composite coatings with high abrasive resistance, Appl. Surf. Sci. 487 (2019) 1329–1340, https://doi.org/10.1016/j.apsusc.2019.05.244.
[167] G. He, S. Lu, W. Xu, T. Yu, J. Li, T. Dai, Durable superhydrophobic Zn/ZnO/TiO_2 surfaces on Ti6Al4V substrate with self-cleaning property and switchable wettability, Ceram. Int. 44 (2018) 638–647, https://doi.org/10.1016/j.ceramint.2017.09.223.
[168] G. Zhao, Y. Xue, Y. Huang, Y. Ye, F. Walsh, J. Chen, S. Wang, One-step electrodeposition of a self-cleaning and corrosion resistant Ni/WS_2 superhydrophobic surface, RSC Adv. 6 (2016) 59104, https://doi.org/10.1039/C6RA07899K.
[169] Y. He, W.T. Sun, S.C. Wang, P.A.S. Reed, F.C. Walsh, An electrodeposited Ni-P-WS_2 coating with combined super-hydrophobicity and self-lubricating properties, Electrochim. Acta 245 (2017) 872–882, https://doi.org/10.1016/j.electacta.2017.05.166.
[170] H.L. Prado, S. Virtanen, Cu–MoS_2 superhydrophobic coating by composite electrodeposition, Coatings 10 (2020), https://doi.org/10.3390/coatings10030238.
[171] G. Zhao, J. Li, Y. Huang, L. Yang, Y. Ye, F.C. Walsh, J. Chen, S. Wang, Robust Ni/WC superhydrophobic surfaces by electrodeposition, RSC Adv. 7 (2017) 44896–44903, https://doi.org/10.1039/C7RA08535D.
[172] J. Tam, J.C.F. Lau, U. Erb, Thermally robust non-wetting Ni-PTFE electrodeposited nanocomposite, Nanomaterials 9 (2018) 9010002, https://doi.org/10.3390/nano9010002.
[173] F. Soleimangoli, S.A. Hosseini, A. Davoodi, A. Mokhtari, M. Alishahi, Effect of NH_4Cl on the microstructure, wettability and corrosion behavior of electrodeposited Ni-Zn coatings with hierarchical nano/microstructure, Surf. Coat. Technol. (2020) 125825, , https://doi.org/10.1016/j.surfcoat.2020.125825.
[174] M. Hashemzadeh, K. Raeissi, F. Ashrafizadeh, S. Khorsand, Effect of ammonium chloride on microstructure, super-hydrophobicity and corrosion resistance of nickel coatings, Surf. Coat. Technol. 283 (2015) 318–328, https://doi.org/10.1016/j.surfcoat.2015.11.008.
[175] J. Ji, W.C. Cooper, D.B. Dreisinger, E. Peters, Surface pH measurements during nickel electrodeposition, J. Appl. Electrochem. 25 (1995) 642–650, https://doi.org/10.1007/BF00241925.
[176] M.-S. Lee, Y.-J. Oh, Chemical equilibria in a mixed solution of nickel and cobalt chloride, Mater Trans 46 (2005) 59–63, https://doi.org/10.2320/matertrans.46.59.
[177] H. Cesiulis, A. Budreika, Electroreduction of Ni (II) and Co (II) from pyrophosphate solutions, Mater. Sci-Medzg 16 (2010), https://www.researchgate.net/publication/228725403.
[178] G. Sazaki, S. Zepeda, S. Nakatsubo, E. Yokoyama, Y. Furukawa, Elementary steps at the surface of ice crystals visualized by advanced optical microscopy, Proc. Natl. Acad. Sci. U.S.A. 107 (2010) 19702–19707, https://doi.org/10.1073/pnas.1008866107.
[179] I.A. Khaddour, L.S.M. Bento, A.M.A. Ferreira, F.A.N. Rocha, Kinetics and thermodynamics of sucrose crystallization from pure solution at different initial supersaturations, Surf. Sci. 604 (2010) 1208–1214, https://doi.org/10.1016/j.susc.2010.04.005.
[180] E. Rahimi, A. Rafsanjani-Abbasi, A. Imani, A.R.K. Rashid, S. Hosseinpour, A. Davoodi, Synergistic effect of a crystal modifier and screw dislocation step defects on the formation mechanism of nickel micro-nanocone, Mater. Lett. 245

(2019) 68–72, https://doi.org/10.1016/j.matlet.2019.02.093.
[181] Z. She, Q. Li, Z. Wang, L. Li, F. Chen, J. Zhou, Researching the fabrication of anticorrosion superhydrophobic surface on magnesium alloy and its mechanical stability and durability, Chem. Eng. J. 228 (2013) 415–424, https://doi.org/10.1016/j.cej.2013.05.017.
[182] T. Xiang, S. Ding, C. Li, S. Zheng, W. Hu, J. Wang, P. Liu, Effect of current density on wettability and corrosion resistance of superhydrophobic nickel coating deposited on low carbon steel, Mater. Des. 114 (2017) 65–72, https://doi.org/10.1016/j.matdes.2016.10.047.
[183] Y. Yang, Y.F. Cheng, Mechanistic aspects of electrodeposition of Ni–Co–SiC composite nano-coating on carbon steel, Electrochim. Acta 109 (2013) 638–644, https://doi.org/10.1016/j.electacta.2013.07.106.
[184] B. Pan, Y. Yao, L. Peng, Q. Zhang, Y. Yang, Ultrasound-assisted pulse electrodeposition of cobalt films, Mater. Chem. Phys. 241 (2020) 122395, , https://doi.org/10.1016/j.matchemphys.2019.122395.
[185] M.S. Chandrasekar, M. Pushpavanam, Pulse and pulse reverse plating—conceptual, advantages and applications, Electrochim. Acta 53 (2008) 3313–3322, https://doi.org/10.1016/j.electacta.2007.11.054.
[186] M. Paunovic, M. Schlesinger, Fundamentals of Electrochemical Deposition, second edition, John Wiley & Sons, New York, 1998, https://doi.org/10.1002/0470009403.
[187] Z. Chen, C. Zhu, M. Cai, X. Yi, J. Li, Growth and morphology tuning of ordered nickel nanocones routed by one-step pulse electrodeposition, Appl. Surf. Sci. 508 (2020) 145291, , https://doi.org/10.1016/j.apsusc.2020.145291.
[188] S. Sangeetha, G.P. Kalaignan, J.T. Anthuvan, Pulse electrodeposition of self-lubricating Ni–W/PTFE nanocomposite coatings on mild steel surface, Appl. Surf. Sci. 359 (2015) 412–419, https://doi.org/10.1016/j.apsusc.2015.10.127.
[189] L. Shen, Y. Wang, W. Jiang, X. Liu, C. Wang, Z. Tian, Jet electrodeposition multilayer nickel on the surface of sintered NdFeB and corrosion behaviours, Corros. Eng. Sci. Technol. 52 (2017) 311–316, https://doi.org/10.1080/1478422X.2016.1278512.
[190] W. Zhuo, L. Shen, M. Qiu, Z. Tian, W. Jiang, Effects of flexible friction on the properties of nanocrystalline nickel prepared by jet electrodeposition, Surf. Coat. Technol. 333 (2018) 87–95, https://doi.org/10.1016/j.surfcoat.2017.10.058.
[191] D. Thiemig, C. Kubeil, C.P. Gräf, A. Bund, Electrocodeposition of magnetic nickel matrix nanocomposites in a static magnetic field, Thin Solid Films 517 (2009) 1636–1644, https://doi.org/10.1016/j.tsf.2008.10.004.
[192] A. Bund, S. Koehler, H.H. Kuehnlein, W. Plieth, Magnetic field effects in electrochemical reactions, Electrochim. Acta 49 (2003) 147–152, https://doi.org/10.1016/j.electacta.2003.04.009.
[193] T.Z. Fahidy, Characteristics of surfaces produced via magnetoelectrolytic deposition, Prog. Surf. Sci. 68 (2001) 155–188, https://doi.org/10.1016/S0079-6816(01)00006-5.
[194] G. Hinds, J.M.D. Coey, M.E.G. Lyons, Influence of magnetic forces on electrochemical mass transport, Electrochem. commun. 3 (2001) 215–218, https://doi.org/10.1016/S1388-2481(01)00136-9.
[195] W. Geng, A. Hu, M. Li, Super-hydrophilicity to super-hydrophobicity transition of a surface with Ni micro–nano cones array, Appl. Surf. Sci. 263 (2012) 821–824, https://doi.org/10.1016/j.apsusc.2012.09.006.
[196] P. Liu, L. Cao, W. Zhao, Y. Xia, W. Huang, Z. Li, Insights into the superhydrophobicity of metallic surfaces prepared by electrodeposition involving spontaneous adsorption of airborne hydrocarbons, Appl. Surf. Sci. 324 (2015) 576–583, https://doi.org/10.1016/j.apsusc.2014.10.170.
[197] I. Tudela, Y. Zhang, M. Pal, I. Kerr, A.J. Cobley, Ultrasound-assisted electrodeposition of composite coatings with particles, Surf. Coat. Technol. 259 (2014) 363–373, https://doi.org/10.1016/j.surfcoat.2014.06.023.
[198] D. Fernandez Rivas, P. Cintas, H.J.G.E. Gardeniers, Merging microfluidics and sonochemistry: towards greener and more efficient micro-sono-reactors, Chem. Commun. (Camb.) 48 (2012) 10935–10947, https://doi.org/10.1039/C2CC33920J.
[199] S. Huang, Y. Hu, W. Pan, Relationship between the structure and hydrophobic performance of Ni–TiO_2 nanocomposite coatings by electrodeposition, Surf. Coat. Technol. 205 (2011) 3872–3876, https://doi.org/10.1016/j.surfcoat.2011.01.065.
[200] I. Tudela, Y. Zhang, M. Pal, I. Kerr, A.J. Cobley, Ultrasound-assisted electrodeposition of thin nickel-based composite coatings with lubricant particles, Surf. Coat. Technol. 276 (2015) 89–105, https://doi.org/10.1016/j.surfcoat.2015.06.030.
[201] S.S. Latthe, R.S. Sutar, A.K. Bhosale, S. Nagappan, C.S. Ha, K.K. Sadasivuni, S. Liu, R. Xing, Recent developments in air-trapped superhydrophobic and liquid-infused slippery surfaces for anti-icing application, Prog. Org. Coat. 137 (2019) 105373, , https://doi.org/10.1016/j.porgcoat.2019.105373.
[202] M. Ruan, W. Li, B. Wang, B. Deng, F. Ma, Z. Yu, Preparation and anti-icing behavior of superhydrophobic surfaces on aluminum alloy substrates, Langmuir 29 (2013) 8482–8491, https://doi.org/10.1021/la400979d.
[203] S. Wang, Z. Yang, G. Gong, J. Wang, J. Wu, S. Yang, L. Jiang, Icephobicity of Penguins Spheniscus humboldti and an artificial replica of penguin feather with air-infused hierarchical rough structures, J. Phys. Chem. C 120 (2016) 15923–15929, https://doi.org/10.1021/acs.jpcc.5b12298.
[204] Y. Cheng, S. Lu, W. Xu, K. Cao, J. Li, Y. Zheng, Controllable fabrication of superhydrophobic alloys surface on copper substrate for self-cleaning, anti-icing, anti-corrosion and anti-wear performance, Surf. Coat. Technol. 333 (2018) 61–70, https://doi.org/10.1016/j.surfcoat.2017.10.069.
[205] S. Zheng, C. Li, Q. Fu, T. Xiang, W. Hu, J. Wang, S. Ding, P. Liu, Z. Chen, Fabrication of a micro-nanostructured superhydrophobic aluminum surface with excellent corrosion resistance and anti-icing performance, RSC Adv. 6 (2016) 79389–79400, https://doi.org/10.1039/C6RA13447E.
[206] W. Hou, Y. Shen, J. Tao, Y. Xu, J. Jiang, H. Chen, Z. Jia, Anti-icing performance of the superhydrophobic surface with micro-cubic array structures fabricated by plasma etching, Colloids Surf, Physicochem. Eng. Aspects 586 (2020) 124180, , https://doi.org/10.1016/j.colsurfa.2019.124180.
[207] L. Tang, N. Wang, Z. Han, H. Sun, D. Xiong, Robust superhydrophobic surface with wrinkle-like structures on AZ31 alloy that repels viscous oil and investigations of the anti-icing property, Colloids Surf, Physicochem. Eng. Aspects 594 (2020) 124655, , https://doi.org/10.1016/j.colsurfa.2020.124655.
[208] Y.L. Zhan, M. Ruan, W. Li, H. Li, L.Y. Hu, F.M. Ma, Z.L. Yu, W. Feng, Fabrication of anisotropic PTFE superhydrophobic surfaces using laser microprocessing and their self-cleaning and anti-icing behavior, Colloids Surf, Physicochem. Eng. Aspects 535 (2017) 8–15, https://doi.org/10.1016/j.colsurfa.2017.09.018.
[209] D. Zang, X. Xun, Z. Gu, J. Dong, T. Pan, M. Liu, Fabrication of superhydrophobic self-cleaning manganese dioxide coatings on Mg alloys inspired by lotus flower, Ceram. Int. 46 (2020) 20328–20334, https://doi.org/10.1016/j.ceramint.2020.05.121.
[210] M. Höök, X. Tang, Depletion of fossil fuels and anthropogenic climate change—a review, Energy Policy 52 (2013) 797–809, https://doi.org/10.1016/j.enpol.2012.10.046.
[211] S.M. Mousavi Ehteshami, S.H. Chan, Techno-economic study of hydrogen production via steam reforming of methanol, ethanol, and diesel, Energy Technol. Policy 1 (2014) 15–22, https://doi.org/10.1080/23317000.2014.933087.
[212] S.K. Saraswat, D.D. Rodene, R.B. Gupta, Recent advancements in semiconductor materials for photoelectrochemical water splitting for hydrogen production using visible light, Renew. Sust. Energ. Rev. 89 (2018) 228–248, https://doi.org/10.1016/j.rser.2018.03.063.
[213] H. Xu, H. Shang, C. Wang, Y. Du, Surface and interface engineering of noble-metal-free electrocatalysts for efficient overall water splitting, Coord. Chem. Rev. 418 (2020) 213374, https://doi.org/10.1016/j.ccr.2020.213374.
[214] Q. Xu, W. Gao, M. Wang, G. Yuan, X. Ren, R. Zhao, S. Zhao, Q. Wang, Electrodeposition of NiS/Ni_2P nanoparticles embedded in amorphous Ni(OH)2 nanosheets as an efficient and durable dual-functional electrocatalyst for overall water splitting, Int. J. Hydrogen Energy 45 (2020) 2546–2556, https://doi.org/10.1016/j.ijhydene.2019.11.217.
[215] J. Ma, X. Tong, J. Wang, G. Zhang, Y. Lv, Y. Zhu, S. Sun, Y.-C. Yang, Y. Song, Rare-earth metal oxide hybridized PtFe nanocrystals synthesized via microfluidic process for enhanced electrochemical catalytic performance, Electrochim. Acta 299 (2019) 80–88, https://doi.org/10.1016/j.electacta.2018.12.132.
[216] C. Cheng, F. Zheng, C. Zhang, C. Du, Z. Fang, Z. Zhang, W. Chen, High-efficiency bifunctional electrocatalyst based on 3D freestanding Cu foam in situ armored CoNi alloy nanosheet arrays for overall water splitting, J. Power Sources 427 (2019) 184–193, https://doi.org/10.1016/j.jpowsour.2019.04.071.
[217] Y. Li, C. Zhao, Enhancing water oxidation catalysis on a synergistic phosphorylated NiFe hydroxide by adjusting catalyst wettability, ACS Catal. 7 (2017) 2535–2541, https://doi.org/10.1021/acscatal.6b03497.
[218] L. Wang, F.S. Xiao, The importance of catalyst wettability, ChemCatChem 6 (2014) 3048–3052, https://doi.org/10.1002/cctc.201402437.
[219] D. Kutyła, A. Salcı, A. Kwiecińska, K. Kołczyk-Siedlecka, R. Kowalik, P. Żabiński, R. Solmaz, Catalytic activity of electrodeposited ternary Co–Ni–Rh thin films for water splitting process, Int. J. Hydrogen Energy (2020), https://doi.org/10.1016/j.ijhydene.2020.05.196.
[220] J. Chen, J. Chen, D. Yu, M. Zhang, H. Zhu, M. Du, Carbon nanofiber-supported PdNi alloy nanoparticles as highly efficient bifunctional catalysts for hydrogen and oxygen evolution reactions, Electrochim. Acta 246 (2017) 17–26, https://doi.org/10.1016/j.electacta.2017.06.047.
[221] Z. Huang, R.S. Gurney, T. Wang, D. Liu, Environmentally durable superhydrophobic surfaces with robust photocatalytic self-cleaning and self-healing properties prepared via versatile film deposition methods, J. Colloid Interface Sci. 527 (2018) 107–116, https://doi.org/10.1016/j.jcis.2018.05.004.
[222] Q. Tan, Z. Gao, J. Yan, D. Xia, W. Hu, Effect of chloride ions in acid and salt solutions on self-repairing ability and corrosion performance of titanium dioxide-fluorosiloxane superhydrophobic coating, Prog. Org. Coat. 146 (2020) 105675, , https://doi.org/10.1016/j.porgcoat.2020.105675.
[223] H.G. Silverman, F.F. Roberto, Understanding marine mussel adhesion, Mar. Biotechnol. 9 (2007) 661–681, https://doi.org/10.1007/s10126-007-9053-x.
[224] H. Lee, S. Dellatore, W. Miller, P. Messersmith, Mussel-inspired surface chemistry for multifunctional coatings, Science 318 (2007) 426–430, https://doi.org/10.1126/science.1147241.
[225] Y. Zhao, J.-B. Xu, J. Zhan, Y.-Q. Chen, J.-M. Hu, Electrodeposited superhydrophobic mesoporous silica films co-embedded with template and corrosion inhibitor for active corrosion protection, Appl. Surf. Sci. 508 (2020) 145242, , https://doi.org/10.1016/j.apsusc.2019.145242.
[226] Y. Li, L. Li, J. Sun, Bioinspired self-healing superhydrophobic coatings, Angew. Chem. Int. Ed. 49 (2010) 6129–6133, https://doi.org/10.1002/anie.201001258.
[227] H. Qian, D. Xu, C. Du, D. Zhang, X. Li, L. Huang, L. Deng, Y. Tu, J.M.C. Mol, H.A. Terryn, Dual-action smart coatings with a self-healing superhydrophobic surface and anti-corrosion properties, J. Mater. Chem. A 5 (2017) 2355–2364, https://doi.org/10.1039/C6TA10903A.